ACS Chemical Neuroscience

pubs.acs.org/chemneuro

Research Article

Knowledge-Based Design of Long-Chain Arylpiperazine Derivatives Targeting Multiple Serotonin Receptors as Potential Candidates for Treatment of Autism Spectrum Disorder

Enza Lacivita,* Mauro Niso, Margherita Mastromarino, Andrea Garcia Silva, Cibell Resch, Andre Zeug, María I. Loza, Marián Castro, Evgeni Ponimaskin, and Marcello Leopoldo*

Cite This: *ACS Chem. Neurosci.* 2021, 12, 1313−1327

Read Online

ACCESS | Metrics & More | Article Recommendations | Supporting Information

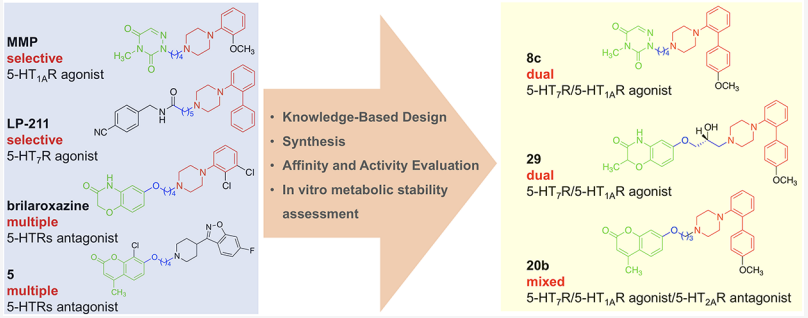

ABSTRACT: Autism spectrum disorder (ASD) includes a group of neurodevelopmental disorders characterized by core symptoms such as impaired social interaction and communication, repetitive and stereotyped behaviors, and restricted interests. To date, there are no effective treatments for these core symptoms. Several studies have shown that the brain serotonin (5-HT) neurotransmission system is altered in both ASD patients and animal models of the disease. Multiple pieces of evidence suggest that targeting 5-HT receptors may treat the core symptoms of ASD and associated intellectual disabilities. In fact, stimulation of the 5-HT_{1A} receptor reduces repetitive and restricted behaviors; blockade of the 5-HT_{2A} receptor reduces both learning deficits and repetitive behavior, and activation of the 5-HT_7 receptor improves cognitive performances and reduces repetitive behavior. On such a basis, we have designed novel arylpiperazine derivatives pursuing unprecedently reported activity profiles: dual 5-HT_7/5-HT_{1A} receptor agonist properties and mixed 5-HT_7 agonist/5-HT_{1A} agonist/5-HT_{2A} antagonist properties. Seventeen new compounds were synthesized and tested in radioligand binding assay at the target receptors. We have identified the dual 5-HT_{1A}R/5-HT_7R agonists **8c** and **29** and the mixed 5-HT_{1A}R agonist/5-HT_7R agonist/5-HT_{2A}R antagonist **20b**. These compounds are metabolically stable in vitro and have suitable central nervous system druglike properties.

KEYWORDS: *5-HT_7 receptor, 5-HT_{1A} receptor, 5-HT_{2A} receptor, arylpiperazine, autism spectrum disorder, knowledge-based design*

INTRODUCTION

Autism spectrum disorder (ASD) includes a group of brain developmental disorders characterized by core symptoms such as impaired social interaction and communication, repetitive and stereotyped behaviors, and restricted interests.[1] In addition, ASD patients often present a variety of additional impairments, including intellectual disability. The frequency of ASD is increasing, with present rates of about 1 in 100 children in Europe and 1 in 54 in the United States.[2] To date, the only drugs approved to treat ASD-related symptoms are the atypical antipsychotics aripiprazole and risperidone (Table 1) which are efficacious to treat irritability, hyperactivity, and aggression but not the core symptoms. Thus, ASD has no cure and its treatment represents a largely unmet clinical need.[3] Several mechanisms have been implicated in ASD, such as synaptic dysfunction (alterations in dendritic spine morphology, excitatory/inhibitory imbalance), neuroinflammation, and altered neurotransmitter systems.[3] Serotonin (5-hydroxytryptamine, 5-HT) exerts a very complex modulatory role in the central nervous system (CNS) involving at least 14 diverse membrane 5-HT receptors (5-HTRs), grouped in seven families (5-HT_{1-7}). 5-HT plays a crucial role in shaping neuronal circuits during prenatal and postnatal development by promoting neurogenesis, neuronal differentiation, axon myelination, neuropil formation, and synaptogenesis.[4,5] Accumulating findings indicate that the

Received: October 9, 2020
Accepted: March 24, 2021
Published: April 1, 2021

Table 1. Structural Formulas and Affinity Profiles of the Reference Compounds

Compound	Structural Formula	K_i [nM] (functional activity)				
		5-HT$_7$	5-HT$_{1A}$	5-HT$_{2A}$	D$_2$	α_{1A}
Aripiprazole[24]	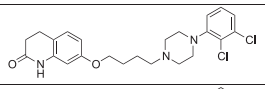	9.6 (weak partial agonist)	5.57 (antagonist)	8.7 (weak partial agonist)	0.66 (antagonist)	26
Brilaroxazine[37]	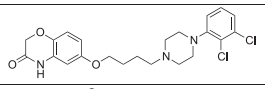	2.7 (antagonist)	1.5 (partial agonist)	2.5 (partial agonist)	0.45 (partial agonist)	NA[a]
WAY-100635[33]	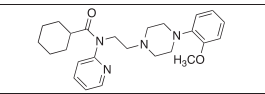	>10,000	2.2 (antagonist)	6260	940	19.9
LP-211[28]	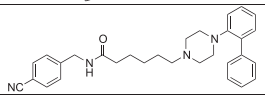	15 (agonist)	379	626	224	22.6
TP-22[32]	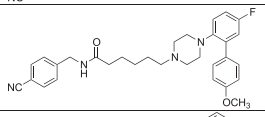	25.5 (agonist)	771	NA	522	6.6
1[29]	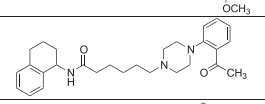	4.14	3.85	12200	68	NA
2[30]	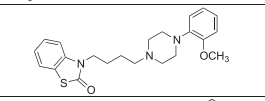	7.7	24.58	NA	NA	NA
3[31]	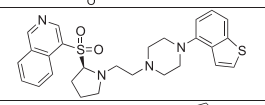	4	24	26	6	NA
4[34]	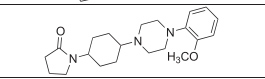	13,000	4 (agonist)	NA	NA	101
MMP[35] **(CUMI-101)**	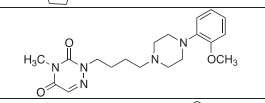	12.9	0.15 (agonist)	4,975	>10,000	6.75
BA-10[18]	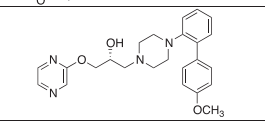	16.1 (agonist)	82.9	NA	NA	NA
UCM-2550[36]	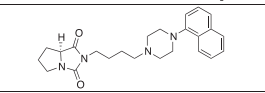	101	4.1 (agonist)	13.5	192	>1000
Risperidone[24]	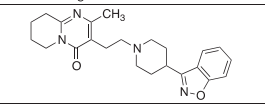	6.6	427.5	0.17	6.5	5
5[38]	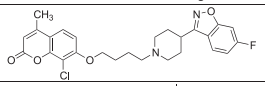	NA	3.3	0.3	2.6	NA
(+)-5-FTP[26]	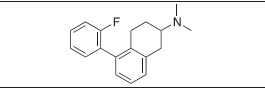	5.8 (antagonist)	22 (partial agonist)	886	>1,000	>10,000

[a]Not Available.

brain 5-HT neurotransmission system is altered in ASD patients[6] and in rodent models of ASD.[7−9] Selective serotonin reuptake inhibitors (SSRIs) have been often prescribed to ASD patients to treat repetitive and stereotyped behaviors as these drugs are efficacious to treat obsessive-compulsive disorder. However, clinical studies in ASD patients treated with SSRIs did not give consistent results.[10] In fact, some studies reported positive effects on stereotypy and compulsions, whereas others reported that SSRIs worsen stereotypy. In addition, side-effects were highly prevalent probably due to the generalized elevation of 5-HT levels that could lead to not therapeutically valid stimulation of multiple 5-HTRs. Various studies have evidenced that targeting certain 5-HTRs has the potential to treat the core symptoms of ASD and associated intellectual disabilities. A clinical trial in young children with ASD demonstrated that the 5-HT$_{1A}$R partial agonist buspirone reduces repetitive and restricted behaviors.[11] Studies in rodent models of ASD have provided further support in this direction. In fact, buspirone and the 5-HT$_{1A}$R full agonist 8-OH-DPAT enhance social interactions.[12,13] The selective 5-HT$_{2A}$R antagonist M100907

https://doi.org/10.1021/acschemneuro.0c00647
ACS Chem. Neurosci. 2021, 12, 1313−1327

Table 2. CNS MultiParameter Optimization (CNS-MPO), Binding Affinities, K_i Ratios, and Microsomal Stability of the Target Compounds

Cmpd	Structure		MPO	K_i [nM] ± S.E.M.				K_i ratio ($^1/_x$)			MS[a] (%)
				5-HT$_7$	5-HT$_{1A}$	5-HT$_{2A}$	D$_2$	5-HT$_{1A}$/5-HT$_7$	5-HT$_{2A}$/5-HT$_7$	5-HT$_{2A}$/5-HT$_{1A}$	
8a	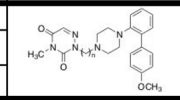	n= 2	5.24	80.0±7.1	1721±110	2350±103	6577±1974[c]	22	29	1.4	17
8b		n= 3	5.32	11.2±0.2	358±30	90.8±34.6	2084±335	32	8.1	0.25 (3.9)	<2
8c		n= 4	4.74	13.0±0.4	3.77±0.02	117±1	508±188	0.3 (3.5)	9	31	28
9	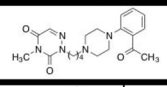		5.82	208±21	6.48±0.70	6730±941[b]	55.8±6.9	0.03 (32)	32	1038	50
11a	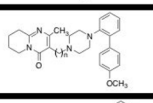	n= 2	3.91	25.6±6.0	289±30	73.5±19.3	592±89	11	2.9	0.25 (4)	21
11b		n= 3	3.64	15.6±2.1	673±131	6.50±1.65	2972±1051	43	0.41 (2.4)	0.01 (100)	14
20a	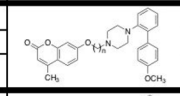	n= 2	3.21	91.7±7.5	1761±127	220±17	301±1	19	2.4	8	<2
20b		n= 3	3.11	47.3±13.7	51.6±12.4	44.9±5.8	330±45	1.1	0.9 (1.1)	0.9 (1.1)	39
20c		n= 4	2.76	42.9±6.5	135±20	54.7±2.3	147±20	3	1.3	0.2 (6)	20
26a	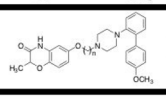	n= 2	3.38	57.2±7.2	1802±420	312±23	541±173	32	5.5	0.2 (6)	28
26b		n= 3	3.30	17.7±2.0	23.2±4.1	130±9	196±9	1.3	7.3	5.6	58
26c[c]		n= 4	2.94	14.7±0.9	127±8	107±1	82.8±6.3	9	7.3	0.65 (1.5)	49
29	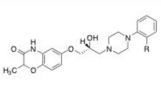	R= 4-MeOPh–	3.44	19.9±1.5	8.70±0.01	141±29	419±141	0.44 (2.3)	7	16	68
30		R= CH$_3$CO–	4.89	46.7±3.7	6.06±0.20	3639±1104	16.8±0.4	0.13 (7.7)	78	600	40
33a	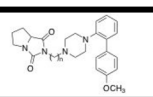	n= 2	5.06	51.6±7.1	1648±202	2218±189	4955±600[c]	32	43	1.3	<2
33b		n= 3	5.20	6.69±1.70	290±17	36.7±11.2	2148±725	43	5.5	8	18
34[c]	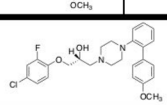		3.04	44.3±7.6	264±8	310±20	845±157	6	7	1.2	34.6

[a]MS: microsomal stability (% of recovery of the parent compound after 30 min incubation with rat microsomes). [b]Full displacement of the specific binding was not achieved at maximum concentration assayed (100 μM); K_i value extrapolated from the analysis might not be accurately estimated; [c]Data from ref 51.

alleviates both learning deficits and repetitive behavior.[14,15] The selective 5-HT$_6$R antagonist SLV reverses the social engagement deficit.[16] The selective 5-HT$_7$R agonist LP-211 (Table 1) corrects behavioral alterations in mouse models of rare neurodevelopmental disorders. In particular, administration of LP-211 (i) improved novel object recognition performance and reduced stereotyped behavior in a mouse model of Fragile-X syndrome (an X-linked disease with autistic features);[17−19] (ii) improved anxiety-related profiles, the exploratory behavior and memory in a mouse model of Rett syndrome (a disease characterized by intellectual disability);[20−22] and (iii) normalized the prepulse inhibition defects observed in a mouse model of CDKL5 deficiency disorder (a disease characterized by severe neurodevelopmental delay impacting cognitive, speech, and visual function).[23] Altogether, the above studies provide support to the search of novel compounds with an appropriate pharmacological profile at 5-HTRs in the prospect to ameliorate the core symptoms of ASD. At present, various examples of drugs or investigational compounds targeting multiple 5-HTRs exist. The most notable examples are aripiprazole (dopamine D$_2$R/5-HT$_{2A}$R/5-HT$_7$R antagonist, 5-HT$_{1A}$R partial agonist) and risperidone (dopamine D$_2$R/5-HT$_{2A}$R/5-HT$_7$R/5-HT$_{1A}$R antagonist) (Table 1).[24] However, aripiprazole and risperidone are not effective on the core symptoms of ASD, suggesting that such particular activity profile is not suitable to treat the core symptoms of ASD.[3] Vortioxetine, a multimodal antidepressant that inhibits 5-HT transporter and activates 5-HT$_{1A}$ and 5-HT$_{1B}$ receptors, suppresses restrictive−repetitive behaviors in a rodent model of ASD but has less efficacy as a sociability enhancer.[25]

These studies strongly suggest the design of new compounds characterized by an activity profile resulting from combinations of activities at 5-HTRs that are predicted to produce effects on the core symptoms of ASD. The first attempt in this direction was reported in 2015 by Canal et al., who developed the compound (+)-5-FPT which was initially described as a high-affinity 5-HT$_7$R and 5-HT$_{1A}$R partial agonist (Table 1). The (+)-5-FPT potently attenuated stereotypy in three heterogeneous models of stereotypy in a mouse strain characterized by repetitive behavior.[26] In 2020, the same research group reported that (+)-5-FPT was actually a 5-HT$_{1A}$R/5-HT$_{2C}$R agonist and 5-HT$_7$R antagonist.[27] This compound was then studied in a mouse model of Fragile X syndrome and found to reduce repetitive behavior through 5-HT$_{1A}$R partial agonism and to attenuate audiogenic seizure through 5-HT$_{2C}$R agonism. Thus, the potential of concomitant activation of 5-HT$_{1A}$R and 5-HT$_7$R was not actually explored.

Therefore, on the basis of the data discussed above, we aimed at identifying completely new modulators of 5-HTRs for studies in the context of ASD. In particular, we searched for (a) a dual 5-HT$_7$R/5-HT$_{1A}$R agonist, which is predicted to increase social interaction through the activation of 5-HT$_{1A}$R and to reduce stereotypy and improve cognition through activation of 5-HT$_7$R, and (b) a compound acting as 5-HT$_7$R/5-HT$_{1A}$R agonist and 5-HT$_{2A}$R antagonist, which is predicted to improve social behavior through activation of 5-HT$_{1A}$R, to reduce or eliminate stereotyped behavior by blocking 5-HT$_{2A}$R, and to improve cognition through activation of 5-HT$_7$R.

https://doi.org/10.1021/acschemneuro.0c00647
ACS Chem. Neurosci. 2021, 12, 1313−1327

Scheme 1. Synthesis of Target Compounds 8a−c and 9[a]

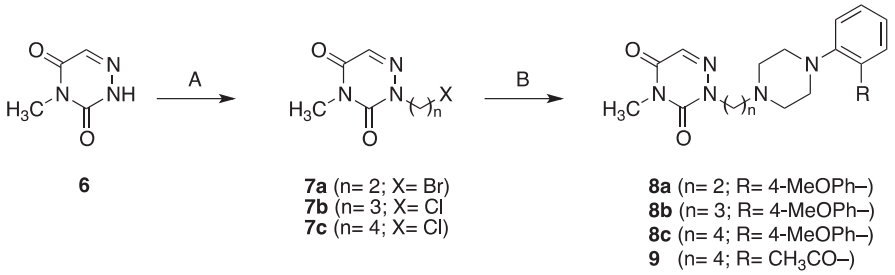

[a]Reagents and conditions: (A) NaH, Br−$(CH_2)_n$−X, anhydrous DMF, rt, 12 h, 40−70% yield; (B) 1-arylpiperazine; K_2CO_3, acetonitrile, reflux overnight, 20−50% yield.

Scheme 2. Synthesis of Target Compounds 11a,b[a]

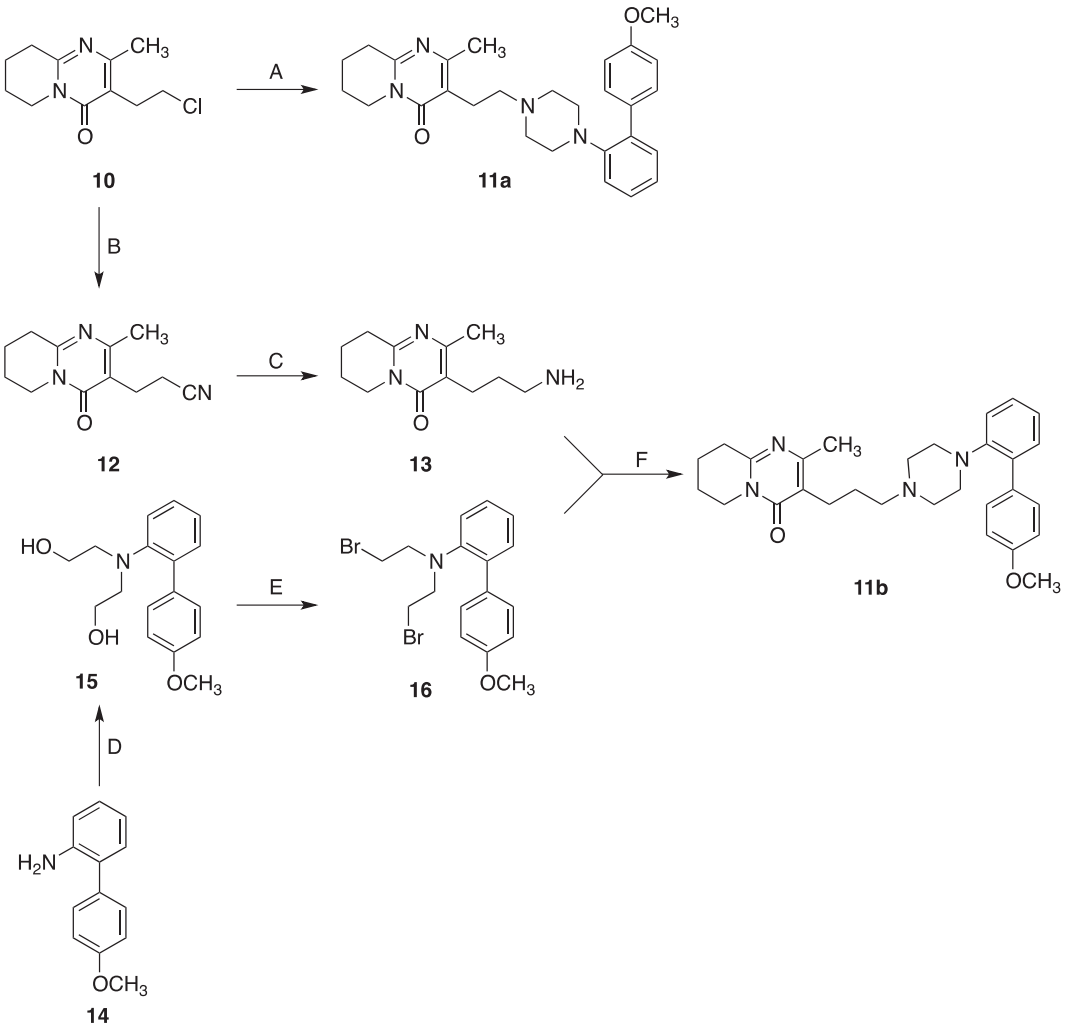

[a]Reagents and conditions: (A) 1-[2-(4-methoxyphenyl)phenyl]piperazine; K_2CO_3, acetonitrile, reflux overnight, 61% yield; (B) NaCN, anhydrous DMF, rt, 5 h, quantitative yield; (C) Raney-nickel, H_2 (4 atm), MeOH, 50% yield; (D) 2-bromoethanol, $CaCO_3$; reflux, 7 h, 37% yield; (E) PBr_3, anhydrous toluene, reflux, 3 h, 65% yield; (F) K_2CO_3, acetonitrile, reflux overnight, 60% yield.

RESULTS AND DISCUSSION

Study Design. Long-chain arylpiperazine derivatives are known to bind monoamine receptors, including 5-HTRs. The general formula is Ar−piperazine−linker−terminal fragment, and it is known that suitable modifications of Ar, linker, or terminal fragment can lead to selective or nonselective compounds. Two examples of selective arylpiperazine ligands are the 5-HT_{1A}R antagonist WAY-100635 and the 5-HT_7R agonist LP-211[28] (Table 1). Instead, compounds **1**[29] and **2**[30] (Table 1) are dual 5-HT_7R/5-HT_{1A}R ligands, and compound **3**[31] is a mixed 5-HT_7R/5-HT_{1A}R/5-HT_{2A}R ligand (Table 1). Thus, long-chain arylpiperazines are a versatile framework to identify compounds with a diversified receptor affinity profile. On the other hand, it appears much less trivial to identify arylpiperazines showing the activity profile that we are pursuing

https://doi.org/10.1021/acschemneuro.0c00647
ACS Chem. Neurosci. 2021, 12, 1313−1327

Scheme 3. Preparation of Target Compounds Featuring the Coumarin Nucleus as the Terminal Fragment[a]

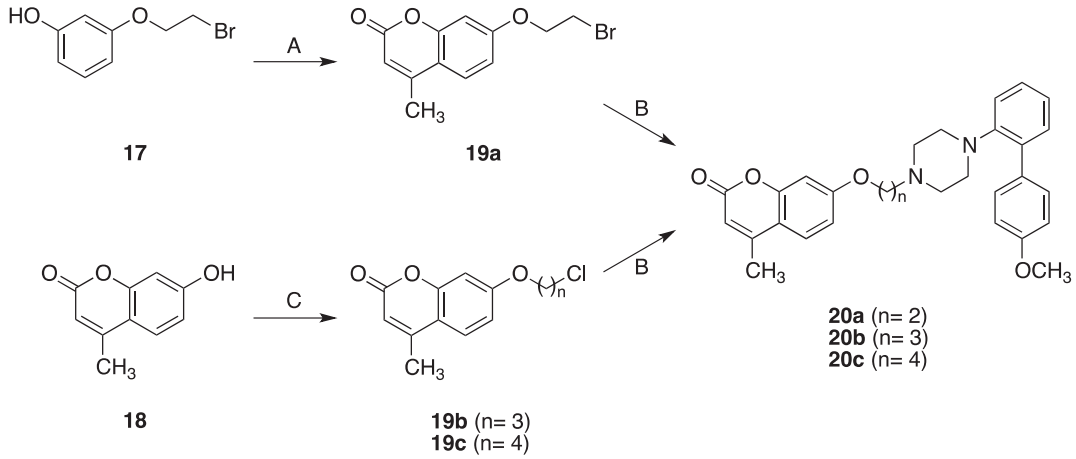

[a]Reagents and conditions: (A) ethyl acetoacetate; conc. H_2SO_4, rt, 4 h, 34% yield; (B) 1-[2-(4-methoxyphenyl)phenyl]piperazine; K_2CO_3, acetonitrile, reflux overnight, 21% yield; (C) NaH, Br−$(CH_2)_n$−X, anhydrous DMF, rt, 12 h, 40−60% yield.

(i.e., dual 5-HT_7R/5-HT_{1A}R agonist, mixed 5-HT_7R agonist/5-HT_{1A}R agonist/5-HT_{2A}R antagonist). To fulfill our aim, we have followed a knowledge-based design (i.e., the collection and reuse of expert knowledge) by selecting Ar groups and terminal fragments present in arylpiperazine-based 5-HTR agonists or antagonists. First, we focused on the Ar group and selected the 1-(biphenyl)piperazine moiety that is the key structural determinant for the agonism at 5-HT_7R of LP-211, TP-22,[32] and BA-10[18] (Table 1). Consequently, the majority of the target compounds are 1-[2-(4-methoxyphenyl)phenyl]piperazine derivatives (see Table 2). In addition, in order to identify dual 5-HT_7R/5-HT_{1A}R ligands, the compounds **9** and **30** (Table 2), featuring the 2-acetylphenyl group present in the dual 5-HT_7R/5-HT_{1A}R ligand **1** (Table 1), were designed. It is worth noting that, even if LP-211, TP-22, and BA-10 are 5-HT_7R-preferring agonists, they still show a measurable affinity for 5-HT_{1A}R (Table 1). Interestingly, LP-211 itself shows measurable 5-HT_{2A}R affinity (Table 1).[28] Thus, the 1-(biphenyl)piperazine framework appears to be compatible with 5-HT_{1A}R and 5-HT_{2A}R affinity, and therefore, suitable variations of the terminal fragments and linkers might increase 5-HT_{1A}R and 5-HT_{2A}R affinity. In the case of 5-HT_{1A}R, the terminal fragment also has a role on the functional activity of the ligand. With this respect, notable examples are the 2-methoxyphenyl piperazine derivatives WAY-100635,[33] **4**,[34] and MMP.[35] In fact, while WAY-100635 is a 5-HT_{1A}R antagonist, compounds **4** and MMP are agonists. Consequently, we have selected the terminal fragments present in the high-affinity 5-HT_{1A}R agonists MMP (which also shows 5-HT_7R affinity in the nanomolar range) and UCM-2550[36] (Table 1). As for 5-HT_{2A}R, we selected the terminal fragments of the antagonists risperidone, brilaroxazine,[37] and **5**[38] (Table 1). Based on the structural similarity with these antagonists, our newly designed arylpiperazine derivatives were expected to act as 5-HT_{2A}R antagonist, as they display a completely different structural motif as compared to that of 5-HT_{2A}R agonists.[39] The fine-tuning of the affinities at the target receptors was accomplished by incorporating 2−5 atom linkers.

In addition, the drug-likeness CNS multiparameter optimization (CNS MPO) algorithm[40] was applied to the designed compounds. As shown in Table 2, 7 out of 17 compounds present a CNS MPO desirability score higher than 4, predictive of alignment to ADME attributes, ability to cross the blood−brain barrier, and low safety risk. As for the remaining compounds, 8 out 10 show CNS MPO desirability score in the range of 3 to 4 which might still include compounds with desirable properties.

In order to evaluate the liability of the target compounds to metabolic degradation by first-pass oxidative metabolism, the main cause of metabolic degradation in vivo, we screened the metabolic stability in vitro by using rat liver microsomes.[41] First, the metabolic stability was assessed as the percentage of the parent compound recovered after 30 min of incubation with microsomes in the presence of an NADPH-regenerating system.[32] Subsequently, selected compounds showing recovery higher than 20% were further characterized by evaluating half-life ($t_{1/2}$) and intrinsic clearance (CL_{int}), which are predictive of in vivo hepatic clearance.

Chemistry. The target compounds **8a−c** and **9** bearing the 4-methyl-1,2,4-triazine-3,5(2*H*,4*H*)-dione moiety as the terminal fragment were prepared according to Scheme 1. 4-Methyl-1,2,4-triazine-3,5(2*H*,4*H*)-dione (**6**)[42] was alkylated with the appropriate haloalkylbromide to give the alkyl halides **7a−c**, which after nucleophilic substitution with the appropriate arylpiperazine, afforded the desired compounds **8a−c** and **9**.

Scheme 2 illustrates the synthesis of target compounds **11a,b**. Compound **11a** was obtained by reacting 3-(2-chloroethyl)-2-methyl-6,7,8,9-tetrahydro-4*H*-pyrido[1,2-*a*]pyrimidin-4-one (**10**)[43] with 1-[2-(4-methoxyphenyl)phenyl]piperazine.[44] Compound **11b** was obtained through a convergent synthesis that required intermediates **13** and **16** (Scheme 2). Amine **13** was synthesized starting from alkyl chloride **10** by sequential reaction with cyanide ion to give the nitrile **12** and reduction of the latter with Raney nickel under hydrogen pressure. Bromide **16** was prepared from 2-(4-methoxyphenyl)aniline (**14**)[44] and 2-bromoethanol in the presence of $CaCO_3$ to afford the bis alkylated product **15**, which was converted into **16** with PBr_3. Condensation of the amine **13** and the bromide **16** yielded the target compound **11b**.

The target compounds featuring the coumarin nucleus as the terminal fragment were prepared as described in Scheme 3. In order to synthesize compound **20a** from compound **19a**, several unsuccessful attempts were made to alkylate 7-hydroxy-4-methylcoumarin (**18**)[45] with 1-bromo-2-chloroethane. Then, compound **19a** was instead synthesized starting from 3-(2-

https://doi.org/10.1021/acschemneuro.0c00647
ACS Chem. Neurosci. 2021, 12, 1313−1327

Scheme 4. Synthetic Route to Obtain Final Compounds 26a[a]

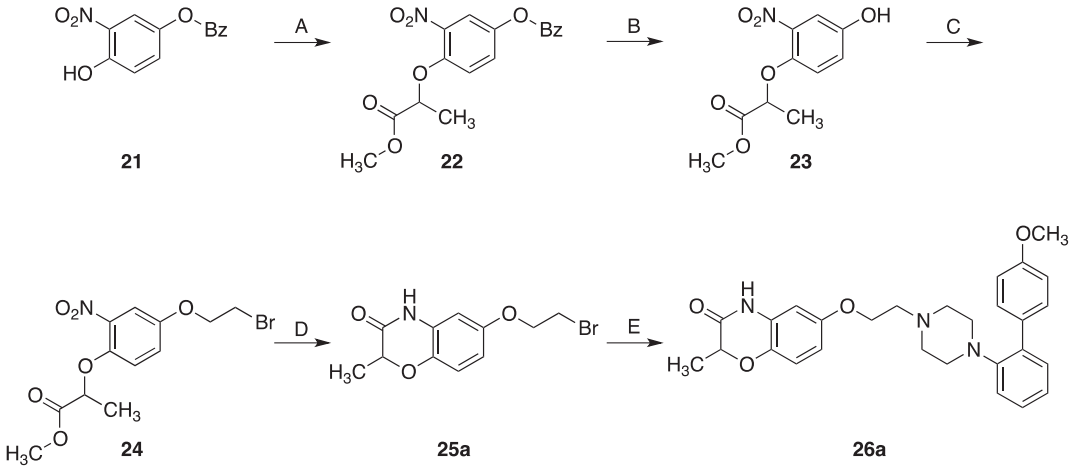

[a]Reagents and conditions: (A) methyl 2-bromopropionate, K_2CO_3, acetone, reflux, 16 h, 54% yield; (B) CH_3ONa, MeOH, rt, 3 h, 89% yield; (C) 1,2-dibromoethane, K_2CO_3, anhydrous DMF, 85 °C, 6 h, 70% yield; (D) Fe dust, AcOH, 80 °C, 1 h, 60% yield; (E) 1-[2-(4-methoxyphenyl)phenyl]piperazine; K_2CO_3, acetonitrile, reflux overnight, 38% yield.

Scheme 5. Synthetic Route to Obtain Final Compounds 26b, 29, and 30[a]

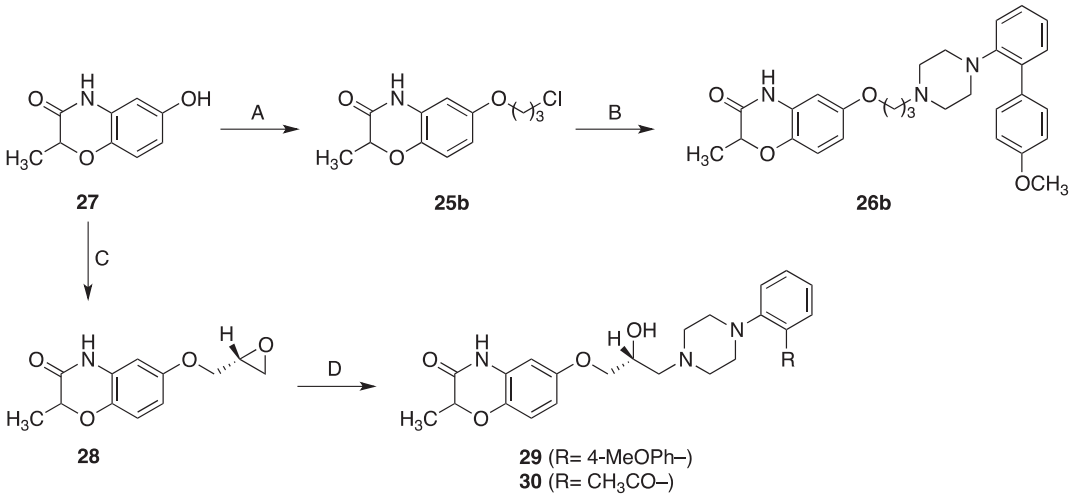

[a]Reagents and conditions: (A) NaH, Br−$(CH_2)_3$−Cl, anhydrous DMF, rt, 24 h, 22−42% yield; (B) 1-[2-(4-methoxyphenyl)phenyl]piperazine; K_2CO_3, acetonitrile, reflux overnight, 20−65% yield. (C) NaH, (*R*)-glycidyl nosilate, anhydrous DMF, rt, overnight, 41% yield; (D) 1-arylpiperazine; EtOH, reflux, 4 h, 30−54% yield.

bromoethoxy)phenol (**17**),[46] which was condensed with ethyl acetoacetate under Pechmann conditions. Nucleophilic substitution of **19a** by 1-[2-(4-methoxyphenyl)phenyl]piperazine afforded the desired compound **20a**. The analogues **20b,c** were prepared starting from phenol **18** which was alkylated with the appropriate bromoalkylchloride to afford derivatives **19b,c**. These latter compounds were condensed with 1-[2-(4-methoxyphenyl)phenyl]piperazine to give the desired compounds **20b,c**, respectively.

The final compounds **26a,b**, **29**, and **30** featuring the benzoxazinone terminal fragment were prepared following two distinct synthetic routes depending on the nature of the linker (Schemes 4 and 5). In fact, the synthesis of the key intermediate **25a** was initially pursued through alkylation of 6-hydroxy-2-methyl-2*H*-benzo[b][1,4]oxazin-3(4*H*)-one (**27**) with 1-bromo-2-chloroethane, but it was unsuccessful. Thus, an alternative synthetic pathway was envisaged (Scheme 4): 4-(benzyloxy)-2-nitrophenol (**21**)[47] was alkylated with methyl 2-bromopropanoate to afford derivative **22**, which was deprotected under basic conditions to give phenol **23**. The latter was alkylated with 1,2-dibromoethane to give **24**. Reduction of the nitro group of **24** by iron dust in acidic conditions resulted in the cyclization of the intermediate amine to give the key intermediate **25a**, which was condensed with 1-[2-(4-methoxyphenyl)phenyl]piperazine to give the target compound **26a**. The other target compound **26b** bearing the benzoxazinone nucleus as terminal fragment was prepared according to Scheme 5. Alkylation of phenol **27**[48] with 1-bromo-3-chloropropane gave the chloroderivative **25b**, which underwent nucleophilic substitution with 1-[2-(4-methoxyphenyl)phenyl]piperazine to give the final compound **26b**. The target compounds **29** and **30** were prepared starting from phenol **27** which was alkylated with (*R*)-glycidylnosilate to give oxirane **28**. Ring opening of **28** with the appropriate 1-arylpiperazine gave **29** and **30**.

The target compounds bearing the tetrahydro-1*H*-pyrrolo-[1,2-*c*]imidazole-1,3(2*H*)-dione as terminal fragment were

https://doi.org/10.1021/acschemneuro.0c00647
ACS Chem. Neurosci. 2021, 12, 1313−1327

Scheme 6. Formation of Target Compounds Bearing the Tetrahydro-1*H*-pyrrolo[1,2-*c*]imidazole-1,3(2*H*)-dione as Terminal Fragment[a]

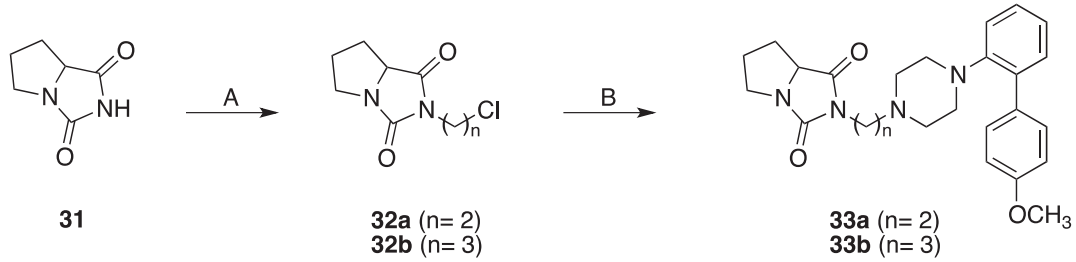

[a]Reagents and conditions: (A) NaH, Br−$(CH_2)_n$−Cl, anhydrous DMF, rt, 12 h, 55−75% yield; (B) 1-[2-(4-methoxyphenyl)phenyl]piperazine; K_2CO_3, acetonitrile, reflux overnight, 43−74% yield.

prepared according to Scheme 6. The *N*-alkylation of hydantoin derivative **31**[49] with the appropriate bromoalkylchloride gave the chloroalkyl intermediates **32a,b**, which were condensed with 1-[2-(4-methoxyphenyl)phenyl]piperazine to afford the desired compounds **33a,b**, respectively.

Binding Affinities to 5-HT$_7$, 5-HT$_{1A}$, 5-HT$_{2A}$, and Dopamine D$_2$ Receptors. All the final compounds were tested in radioligand binding assays to determine their affinity for 5-HT$_7$R, 5-HT$_{1A}$R, and 5-HT$_{2A}$R (Table 2). In addition, the compounds were counter screened at dopamine D$_2$ receptors, because blockade of this receptor may cause motor dysfunctions.[50] The assays were performed via the displacement of the specific binding of [^{3}H]-5-CT (for 5-HT$_7$R), [^{3}H]-8-OH-DPAT (for 5-HT$_{1A}$R), [^{3}H]ketanserin (for 5-HT$_{2A}$R), and [^{3}H]-spiperone (for dopamine D$_2$ receptor), at the cloned human receptors stably expressed in HEK293 cells (5-HT$_7$R, 5-HT$_{1A}$R) or CHO-K1 cells (5-HT$_{2A}$R, D$_2$ receptor).

The K_i values at 5-HT$_7$R of the target 1-[2-(4-methoxyphenyl)phenyl]piperazine derivatives **8a,b**, **11a,b**, **20a−c**, **26a−c**, **29**, and **33a,b** are in the range 6.69−91.7 nM, indicating that the structural variations introduced to the terminal fragment or linker of LP-211 were well tolerated. In fact, such variations translate into small changes in affinity, the largest variation being in the case of **33a** and **33b** (7-fold). Of note, the 5-HT$_7$R affinity values of the reference compounds brilaroxazine (vs **26a−c**, **29**), UCM-2550 (vs **33a,b**), risperidone (vs **11a,b**), and MMP (vs **8a−c**) fell in the same range. Instead, the 1-(2-acetylphenyl)piperazine derivatives **9** and **30** were 50- and 11-fold less potent than the reference compound **1** at 5-HT$_7$R.

As for the 5-HT$_{1A}$R affinities, the 1-(2-acetylphenyl)-piperazine derivatives **9** and **30** were equipotent potent to the reference compound **1**, whereas the target 1-[2-(4-methoxyphenyl)phenyl]piperazine derivatives **8a,b**, **11a,b**, **20a−c**, **26a−c**, **29**, and **33a,b** showed K_i values distributed in a wide range (3.77−1802 nM), as the result of a more pronounced impact of the linker length. In fact, the 4-methyl-1,2,4-triazine-3,5(2*H*,4*H*)-dione derivative **8c** displays K_i = 3.77 nM, whereas its shorter homologue **8a** shows a 456-fold lower 5-HT$_{1A}$R affinity. Similarly, the benzoxazinone derivative **26b** displays K_i = 23.2 nM, whereas its shorter homologue **26a** shows 78-fold lower affinity. The comparison of the close analogs **26a−c**, **29**, and **34** provides an interesting example of how the affinity for 5-HT$_7$R and 5-HT$_{1A}$R can be fine-tuned by the nature of the terminal fragment and the linker. It can be noted that the target compounds **26a−c**, **29** (vs brilaroxazine), **33a,b** (vs UCM-2550), **8a−c** (vs MMP), and **20a−c** (vs **5**) display lower 5-HT$_{1A}$R affinity than that of the reference compounds featuring the corresponding terminal fragment. Nonetheless, the proposed structural changes led to the identification of six compounds (**8c**, **11a**, **20b**, **26b,c**, and **33b**) with 5-HT$_{1A}$R affinity higher than that of LP-211.

Considering the affinity at 5-HT$_{2A}$R, all the target 1-[2-(4-methoxyphenyl)phenyl]piperazine derivatives show affinity higher than that of LP-211, except **8a** and **33a**, confirming the validity of the selection of terminal fragments present in the reference compounds. Compounds **8a** and **33a** represent an unfavorable combination of linker length and terminal fragment. The most pronounced increase was in the case of compound **11b** in which the terminal fragment is the same as in risperidone. The 5-HT$_{2A}$R affinity of the final 1-(2-acetylphenyl)piperazine derivatives **9** and **30** was in the micromolar range, which was similar to the affinity value of the corresponding reference compound **1**.

The D$_2$ receptor affinities of the target 1-[2-(4-methoxyphenyl)phenyl]piperazine derivatives were all lower than that of LP-211, but **26c** that displayed a K_i value lower than 100 nM. Most importantly, the reference compounds risperidone (vs **11a,b**), **5** (vs **20a−c**), brilaroxazine (vs **26a−c**, **29**), and UCM-2550 (vs **33a,b**) show higher D$_2$ receptor affinity than that of the target compounds featuring the corresponding terminal fragment. Thus, the affinity of the target compounds at D$_2$ receptors seems to be determined by the 1-[2-(4-methoxyphenyl)phenyl]piperazine moiety rather than the linker length and the terminal fragment. As for the 1-(2-acetylphenyl)-piperazine derivatives **9** and **30**, both compounds showed high D$_2$ receptor affinity, being the most potent D$_2$ receptor ligands among the newly synthesized compounds.

Next, in order to select dual 5-HT$_7$R/5-HT$_{1A}$R or mixed 5-HT$_7$R/5-HT$_{1A}$R/5-HT$_{2A}$R ligands, we analyzed the 5-HT$_{1A}$R/5-HT$_7$R, 5-HT$_{2A}$R/5-HT$_7$R, and 5-HT$_{2A}$R/5-HT$_{1A}$R K_i ratios (Table 2). As reference values, we selected the K_i ratios of compound **26c** which, according to our recent study, behaved as a 5-HT$_7$R-preferring agonist in vitro and in vivo.[51] Consequently, to select the dual 5-HT$_{1A}$R/5-HT$_7$R ligands, we considered compounds showing a 5-HT$_{1A}$R/5-HT$_7$R K_i ratio lower than 9 (and greater than 0.11, i.e., the reciprocal of 9). Compounds **8c**, **29**, and **30** displayed such characteristic. These compounds were also selective over 5-HT$_{2A}$R. The most balanced 5-HT$_{1A}$R/5-HT$_7$R ligands of this set were **8c** and **29**, as they showed the 5-HT$_7$R/5-HT$_{1A}$R K_i ratios closest to 1. On the other hand, compounds **20b**, **20c**, **26b**, and **34** displayed mixed 5-HT$_7$R/5-HT$_{1A}$R/5-HT$_{2A}$R affinity, with **20b** being the compound with the most balanced affinity profile (all three K_i ratios close to 1).

https://doi.org/10.1021/acschemneuro.0c00647
ACS Chem. Neurosci. 2021, 12, 1313−1327

In Vitro Metabolic Stability. The aim of this study is to provide the scientific community with molecules suitable for studies in vivo. In order to predict the extent of first-pass oxidative metabolism, the target compounds were incubated with rat liver microsomes in the presence of an NADPH regenerating system.[41] In the initial screening phase, we assessed the percentage of the parent compound recovered after 30 min of incubation. The percentages of recovery of LP-211 and TP-22 were 20 and 27%, respectively,[32] which represented the reference values to compare the new compounds. As it can be seen in Table 1, the majority of the new compounds show in vitro stability higher than LP-211, as 11 out of 17 compounds display a percentage of recovery >20%. Then, taking into account the affinity, selectivity, and metabolic stability data, we assessed the half-life and the intrinsic clearance in vitro of compounds **8c**, **20b,c**, **26a,b**, and **29** (Table 3). The data indicate that all the selected compounds showed higher stability than that of LP-211, with intrinsic clearance values lower up to 5-fold as in the case of compound **29**. Thus, the compounds listed in Table 3 are predicted to be low-clearance compounds and suitable for studies in vivo.[52] These results provide further support to the strategy of using structural motifs featured by druglike compounds to obtain metabolically stable compounds.[40,51]

Table 3. Half-Life ($t_{1/2}$) and Intrinsic Clearance (CL_{int}) of Selected Compounds

compound	$t_{1/2}$ (min)	CL_{int} (μL/mg/min)
LP-211[32]	15	45.9
TP-22[32]	45	16.1
8c	41	16.9
20b	39	17.7
20c	23	30
26a	49	14.1
26b	60	11.5
26c[51]	63	11
29	74	9.4
34[51]	58	12

The metabolic stability and the affinity data supported the selection of the dual 5-HT_7R/5-HT_{1A}R ligands **8c** and **29** and the mixed 5-HT_7R/5-HT_{1A}R/5-HT_{2A}R ligand **20b** for further evaluations. These compounds distinguished themselves from the reference compounds for the binding profile at 5-HT_7, 5-HT_{1A}, 5-HT_{2A}, and D_2 receptors. As shown in Table 1, most of the reference compounds display an affinity for α_{1A} adrenoceptor, and therefore, it was not unexpected that compounds **8c**, **20b**, and **29** showed α_{1A} adrenoceptor affinity (K_i= 23.5, 66.1, and 55.8 nM, respectively, see Supporting Information). In fact, the search for arylpiperazine derivatives with affinity for multiple 5-HTRs might imply that the compounds have an affinity for other monoamine receptors (see Supporting Information for off-target affinities of compounds **8c**, **20b**, and **29**). Considering that α_{1A} adrenoceptor activity might cause cardiovascular side-effect, this particular off-target activity is a safety warning for future developments of this class of compounds.

Functional Activities at 5-HT_7R, 5-HT_{1A}R, and 5-HT_{2A}R of Compounds 8c, 20b, and 29. To provide a functional analysis at 5-HT_7R, the cAMP response mediated by **8c**, **20b**, **29** and the reference 5-HT_7R agonists 5-CT and LP-211[29,53] was analyzed. To this end, 5-HT_7R-mCherry was coexpressed with the FRET-based cAMP biosensor CEPAC.[54] This biosensor includes the cAMP-binding domain of the EPAC protein cloned between mCerulean (FRET donor) and Citrine (FRET acceptor). Upon cAMP binding, conformational changes of the sensor occur, leading to a decrease in the FRET signal

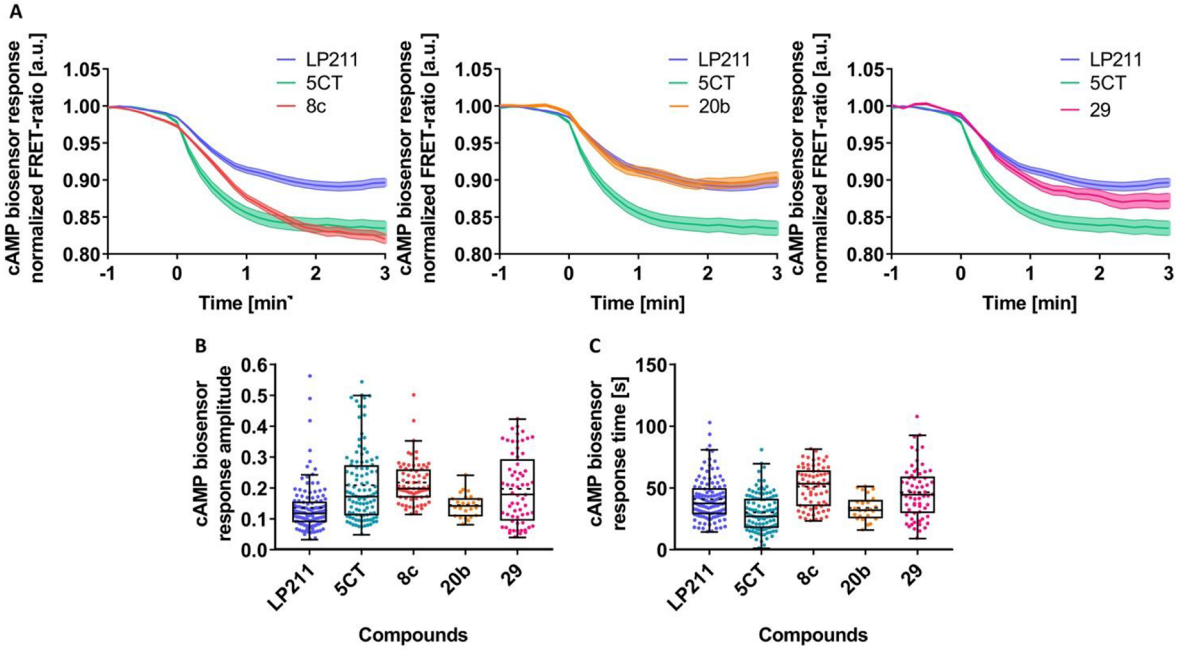

Figure 1. Compounds **8c**, **20b**, and **29** stimulate 5-HT_7R-mediated cAMP production. (A) N1E cells were transfected with cAMP FRET-based biosensor CEPAC and 5-HT_7R-mCherry. Cells were stimulated with the compounds, as indicated. Mean values of the cAMP-biosensor response upon stimulation with **8c** **20b**, and **29** are shown. Stimulation with LP-211 and 5-CT was used as a control. (B) Quantification of the response amplitude and (C) response time shown as the mean ± SEM ($3 < N < 6$, in each experiment at least 20 cells were analyzed).

https://doi.org/10.1021/acschemneuro.0c00647
ACS Chem. Neurosci. 2021, 12, 1313−1327

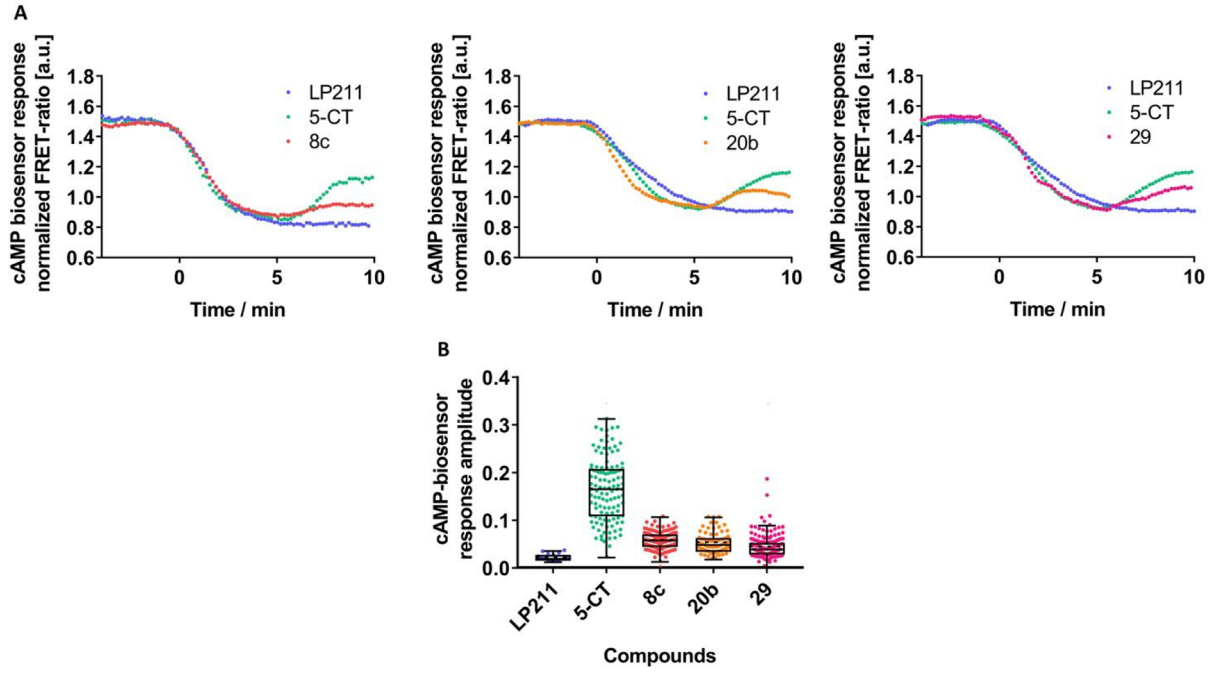

Figure 2. Compounds **8c**, **20b**, and **29** behave as 5-HT$_{1A}$R agonists in the receptor-mediated cAMP inhibition. (A) N1E cells were transfected with cAMP FRET-based biosensor CEPAC and 5-HT$_{1A}$R-mCherry. After pretreatment with 1 μM forskolin and 25 μM IBMX, cells were stimulated with the indicated compounds. Each trace shows cAMP response at the single cell. (B) Graphs show changes of cAMP response amplitude relative to pretreatment (mean ± SEM, 3 < N < 6, in each experiment at least 20 cells were analyzed).

(Figure 1A). The cAMP responses were recorded at the single-cell level by monitoring the CEPAC fluorescence intensity ratio of the acceptor to the donor (A/D ratio). The strength and speed of serotonergic signaling was determined from the amplitude and time dependence of the CEPAC fluorescence intensity ratio.

In the absence of 5-HT$_7$R, no cAMP response was observed upon treatment with the ligands (data not shown). In contrast, in cells expressing 5-HT$_7$R, all the compounds (10 μM) were able to increase the intracellular cAMP level, although with different efficiencies. Statistical analysis by fitting the experimental data to the single exponential revealed that **8c** and **29** elicited the largest cAMP response amplitude compared with that of 5-CT, followed by **20b** (Figure 1A). Of note, response amplitude for all compounds tested was higher than that measured for highly selective 5-HT$_7$R agonist LP-211 (Figure 1B). The mean response times for all compounds were higher (i.e., slower response kinetics) than that obtained for 5-CT and comparable with the values obtained for LP-211 (Figure 1C).

We next analyzed whether **8c**, **20b**, and **29** would affect the 5-HT$_{1A}$R function toward cAMP inhibition. The 5-HT$_{1A}$R agonist 5-CT was used as a positive control,[55] while LP-211 (selective 5-HT$_7$R agonist) was used as a negative control. To this end, 5-HT$_{1A}$R-mCherry was coexpressed with the CEPAC biosensor in N1E cells. We subsequently analyzed the ability of 5-HT$_{1A}$R-mediated signaling via Gi to inhibit the forskolin (FSK)-induced cAMP accumulation following receptor stimulation with above-mentioned compounds (10 μM). Except for LP-211 treatment, an increase of the A/D ratio of CEPAC was observed in all the cases, that indicated the 5-HT$_{1A}$R-mediated downregulation of intracellular concentration of cAMP (Figure 2). Statistical evaluation of amplitudes of the cAMP decay for **8c**, **20b**, and **29** revealed that, although these compounds were still able to evoke receptor-mediated decrease of the concentration of cAMP, they were less effective in activation of 5-HT$_{1A}$R when compared with 5-CT (Figure 2B).

Finally, compounds **8c**, **20b**, and **29** were investigated in functional assays of 5-HT$_{2A}$R-mediated inositol phosphate (IP) signaling in CHO-K1 cells expressing the cloned human receptor. The three compounds, in concentration−response curves from 1 nM to 100 μM, fully antagonized in a concentration-dependent manner the stimulation of IP production elicited by 1 μM 5-HT (Figure 3). Consistently, no agonist activity was observed for **20b** at the same concentrations in these assays (data not shown). IC$_{50}$ values were similar for the three compounds and in the nanomolar range, consistent with their affinities at 5-HT$_{2A}$R (IC$_{50}$ = 595, 666, and 491 nM for **8c**, **20b**, and **29**, respectively). The

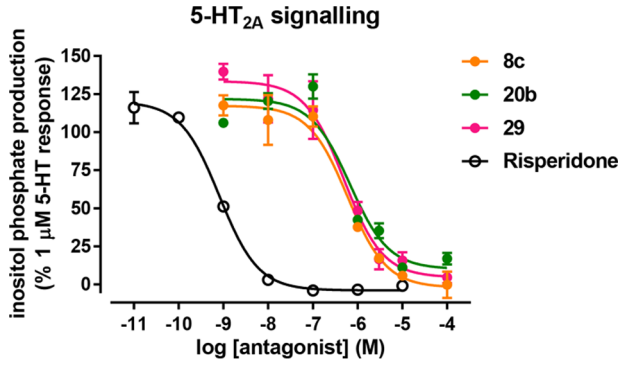

Figure 3. Functional assays of inositol phosphate (IP) signaling at cloned human 5-HT$_{2A}$Rs. Concentration−response inhibition curves of **8c**, **20b**, **29**, and risperidone (as reference 5-HT$_{2A}$R antagonist) on IP production stimulated by 1 μM 5-HT in CHO-K1 cells expressing human 5-HT$_{2A}$Rs. The graph shows data (mean ± SEM) from one experiment performed in duplicate.

https://doi.org/10.1021/acschemneuro.0c00647
ACS Chem. Neurosci. 2021, 12, 1313−1327

reference 5-HT_{2A}R antagonist risperidone (0.01 nM−10 μM) showed a IC_{50} value of 0.81 nM (Figure 3).

Collectively, the functional activities of the selected compounds supported the validity of the design approach. In fact, compounds **8c**, **20b**, and **29** behave as 5-HT_7R agonists in the same way as LP-211−confirming that the 1-(biphenyl)-piperazine moiety is a key structural determinant for 5-HT_7R agonism and as 5-HT_{2A}R antagonists as various other arylpiperazine derivatives. As for 5-HT_{1A}R, the comparison of the functional activities of **8c**, **20b**, and **29** with LP-211 suggest that the 1-(biphenyl)piperazine moiety alone is not responsible for the functional activity at 5-HT_{1A}R, which, instead, is determined also by the nature of the terminal fragment and linker length, as already noted in the Study Design paragraph.

CONCLUSIONS

5-HT neurotransmission system is an active area of investigation in ASD research. Several in vitro and in vivo studies with selective 5-HTR agonists or antagonists have suggested that targeting a subpopulation of the 5-HTRs might alleviate the core symptoms of ASD. Based on the current knowledge, we aimed at identifying a dual 5-HT_7R/5-HT_{1A}R agonist and a mixed 5-HT_7R/5-HT_{1A}R agonist/5-HT_{2A}R antagonist. A set of novel arylpiperazine derivatives were designed by exploiting structural motifs that might drive the functional activity of the target compounds toward the desired profile (knowledge-based design). The design strategy succeeded as we identified compounds **8c** and **29** that are 5-HT_7R and 5-HT_{1A}R preferring agonists and compound **20b**, a mixed 5-HT_7R/5-HT_{1A}R agonist/5-HT_{2A}R antagonist with almost identical affinity for the three receptors. The knowledge-based design strategy had a favorable influence on the in vitro pharmacokinetic properties of most of the newly designed compounds. In fact, **8c**, **20b**, and **29** are metabolically stable in vitro and also have suitable CNS druglike properties. Considering the complex mechanisms underlying ASD, we believe that a polypharmacology approach might be more suited than a single target approach. We hope that pharmacological tools such as **8c**, **20b**, and **29** will contribute to the progress of the discovery of drugs for ASD.

METHODS

Chemistry. Chemicals were purchased from Sigma-Aldrich, Alfa Aesar, TCI Chemicals. Unless otherwise stated, all chemicals were used without further purification. Thin layer chromatography (TLC) was performed using plates from Merck (silica gel 60 F254). Column chromatography was performed with 1:30 Merck silica gel 60 Å (63−200 μm) as the stationary phase. Flash chromatographic separations were performed on a Biotage SP1 purification system using flash cartridges prepacked with KP-Sil 32−63 μm, 60 Å silica. ^{1}H NMR spectra were recorded on a Varian Mercury-VX spectrometer (300 MHz) or on a 500-vnmrs500 Agilent spectrometer (500 MHz). All chemical shift values are reported in parts per million (ppm, δ). Splitting patterns are designated as follows: app (apparent), br (broad), s (singlet), d (doublet), t (triplet), q (quartet), dd (doublet of doublets), td (triplet of doublets). For target compounds, NMR spectra were recorded on free bases. Recording of mass spectra was done on an HP6890-5973 MSD gas chromatograph/mass spectrometer; only significant m/z peaks, with their percentage of relative intensity in parentheses, are reported. ESI-MS/MS analyses were performed with an Agilent 1100 Series LC-MSD trap System VL workstation, mass range 50−800 m/z, electrospray ion source in positive or negative ion mode. All spectra were in accordance with the assigned structures. Elemental analysis (C,H,N) of the target compounds as hydrochloride salts were performed on a Eurovector Euro EA 3000 analyzer. Analyses indicated by the symbols of the elements were within ±0.4% of the theoretical values. The purity of the target compounds listed in Table 2 was assessed by RP-HPLC and combustion analysis. All compounds showed ≥95% purity. RP-HPLC analysis was performed on an Agilent 1260 Infinity Binary LC System equipped with a diode array detector using a Phenomenex Gemini C-18 column (250 mm × 4.6 mm, 5 μm particle size). All target compounds (Table 2) were eluted with CH_3CN/ammonium formate 50 mM pH 5, 8:2 (v/v) at a flow rate of 1 mL/min. All compounds showed ≥95% purity.

The following compounds were prepared as described in the literature: 1-[2-(4-methoxyphenyl)phenyl]piperazine;[46] 1-(2-(piperazin-1-yl)phenyl)ethanone;[56] 4-methyl-1,2,4-triazine-3,5(2*H*,4*H*)-dione (**6**);[43] 2-(4-chlorobutyl)-4-methyl-1,2,4-triazine-3,5(2*H*,4*H*)-dione (**7c**);[43] 3-(2-chloroethyl)-2-methyl-6,7,8,9-tetrahydro-4*H*-pyrido[1,2-*a*]pyrimidin-4-one (**10**);[44] 4′-methoxy-[1,1′-biphenyl]-2-amine (**14**);[46] 3-(2-bromoethoxy)phenol (**17**);[45] 7-hydroxy-4-methylchromen-2-one (**18**);[47] 4-(benzyloxy)-2-nitrophenol (**21**);[48] 6-[3-[4-[2-(4-methoxyphenyl)phenyl]piperazin-1-yl]butoxy]-2-methyl-2*H*-benzo[b][1,4]oxazin-3(4*H*)-one (**26c**);[51] 6-hydroxy-2-methyl-2*H*-benzo[*b*][1,4]oxazin-3(4*H*)-one (**27**);[49] tetrahydro-1*H*-pyrrolo[1,2-*c*]imidazole-1,3(2*H*)-dione (**31**);[50] (*R*)-1-(4-chloro-2-fluorophenoxy)-3-[4-[2-(4-methoxyphenyl)phenyl]piperazin-1-yl]propan-2-ol (**34**).[51] Complete synthetic procedures and intermediated spectroscopic data are fully reported in the Supporting Information.

General Procedure for the Preparation of Target Compounds 8a−c, 9, 11a,b, 20a−c, 26a,b, and 33a,b. A stirred mixture of the appropriate alkylating agent (0.7 mmol), 1-[2-(4-methoxyphenyl)phenyl]piperazine or 1(2-acetylphenyl)piperazine (0.84 mmol), and K_2CO_3 (0.1 g, 0.7 mmol) in acetonitrile (20 mL) was refluxed overnight. After cooling, the mixture was evaporated to dryness, and H_2O (20 mL) was added to the residue. The aqueous phase was extracted with AcOEt (2 × 30 mL). The collected organic layers were dried over Na_2SO_4 and evaporated under reduced pressure. The crude residue was purified by chromatographic column as detailed below to afford pure target compound.

*2-{4-[4-[2-(4-Methoxyphenyl)phenyl]piperazin-1-yl]ethyl}-4-methyl-1,2,4-triazine-3,5(2H,4H)-dione (**8a**).* Eluted with $CHCl_3$/MeOH, 98:2. Yellow oil, 73% yield. ^{1}H NMR ($CDCl_3$): δ 2.43 (br s, 4H), 2.67 (t, 2H, J = 6.6 Hz), 2.80 (br s, 4H), 3.32 (s, 3H), 3.85 (s, 3H), 4.08 (t, 2H, J = 6.6 Hz), 6.91−6.93 (m, 2H), 7.00 (d, 1H, J = 7.8 Hz), 7.04 (td, 1H, J = 1.1 and 7.6 Hz), 7.21 (dd, 1H, J = 1.5 and 7.3 Hz), 7.26 (m, 1H), 7.37 (s, 1H), 7.55−7.57 (m, 2H). GC/MS m/z 422 (M^+, 4), 421 (M^+, 16), 281 (100). Anal. ($C_{23}H_{27}N_5O_3$·HCl·H_2O) C, H, N.

*2-{3-[4-[2-(4-Methoxyphenyl)phenyl]piperazin-1-yl]propyl}-4-methyl-1,2,4-triazine-3,5(2H,4H)-dione (**8b**).* Eluted with $CHCl_3$/EtOAc, 1:1. Brown oil, 40% yield. ^{1}H NMR ($CDCl_3$): δ 1.88−1.92 (m, 2H), 2.34 (br s, 4H), 2.40 (t, 2H, J = 7.0 Hz), 2.80 (br s, 4H), 3.32 (s, 3H), 3.85 (s, 3H), 4.03 (t, 2H, J = 7.0 Hz), 6.92 (d, 2H, J = 8.8 Hz), 6.98−7.05 (m, 2H), 7.02−7.07 (m, 1H), 7.19−7.22 (m, 1H), 7.36 (s, 1H), 7.56 (d, 2H, J = 8.8 Hz). GC/MS m/z 436 (M^+ + 1, 20), 435 (M^+, 100), 281 (70), 212 (57), 167 (34). Anal. ($C_{24}H_{29}N_5O_3$·HCl·H_2O) C, H, N.

*2-{2-[4-[2-(4-Methoxyphenyl)phenylpiperazin-1-yl]butyl}-4-methyl-1,2,4-triazine-3,5(2H,4H)-dione (**8c**).* Eluted with $CHCl_3$/MeOH, 95:5. Pale yellow oil, 30% yield. ^{1}H NMR ($CDCl_3$): δ 1.47 (m, 2H), 1.71−1.80 (m, 2H), 2.34 (app t, 6H), 2.85 (app t, 4H), 3.33 (s, 3H), 3.98 (t, 2H, J = 7.0 Hz), 6.91−6.95 (m, 2H), 7.00−7.07 (m, 2H), 7.29−7.24 (m, 2H), 7.37 (s, 1H), 7.55−7.59 (m, 2H). ^{13}C NMR (500 MHz, $CDCl_3$): δ 158.7; 155.9; 148.9; 147.7; 134.9; 134.3; 132.7; 131.5; 129.9; 128.36; 124.3; 118.9; 113.8; 124.2; 118.7; 113.8; 55.3; 52.4; 50.5; 47.7; 27.1. ESI-MS m/z 472 (M + Na)$^+$. ESI-MS/MS m/z 323 (100). Anal. ($C_{25}H_{31}N_5O_3$·HCl) C, H, N.

*2-[4-[4-(2-Acetylphenyl)piperazin-1-yl]butyl]-4-methyl-1,2,4-triazine-3,5(2H,4H)-dione (**9**).* Eluted with $CHCl_3$/MeOH, 98:2. Yellow oil, 20% yield. ^{1}H NMR ($CDCl_3$): δ 1.57 (m, 2H), 1.81 (m, 2H), 2.44 (t, 2H, J = 7.6 Hz), 2.60 (br s, 4H), 2.65 (s, 3H), 3.02 (app. t, 4H), 3.35 (s, 3H), 4.02 (t, 2H, J = 7.1 Hz), 7.04−7.08 (m, 2H), 7.39−7.42 (m, 3H). GC/MS m/z 386 (M^+ + 1, 10), 385 (M^+, 30), 237 (90), 207 (100), 161 (95). Anal. ($C_{20}H_{27}N_5O_3$·2HCl) C, H, N.

*3-{2-[4-[2-(4-Methoxyphenyl)phenyl]piperazin-1-yl]ethyl}-2-methyl-6,7,8,9-tetrahydro-4H-pyrido[1,2-a]pyrimidin-4-one (**11a**).*

https://doi.org/10.1021/acschemneuro.0c00647
ACS Chem. Neurosci. 2021, 12, 1313−1327

Eluted with $CHCl_3$/MeOH, 98:2. Brown solid, 60% yield. ^{1}H NMR ($CDCl_3$): δ 1.84−1.89 (m, 2H), 1.92−1.97 (m, 2H), 2.27 (s, 3H), 2.45−2.50 (m, 6H), 2.69−2.72 (br t, 2H), 2.85 (t, 2H, J = 6.8 Hz), 2.89 (br s, 4H), 3.85 (s, 3H), 3.91 (t, 2H, J = 6.1 Hz), 6.90−6.93 (m, 2H), 7.03−7.06 (m, 2H), 7.21 (dd, 1H, J = 1.5 and 7.3 Hz), 7.25 (td, 1H, J = 1.5 and 7.8 Hz), 7.55−7.58 (m, 2H). GC/MS m/z 458 (M^+, 2), 281 (100). Anal. ($C_{28}H_{34}N_4O_2$·2HCl) C, H, N.

*3-{3-[4-[2-(4-Methoxyphenyl)phenyl]piperazin-1-yl]propyl}-2-methyl-6,7,8,9-tetrahydro-4H-pyrido[1,2-a]pyrimidin-4-one (**11b**).* Eluted with $CHCl_3$/EtOAc, 1:1. Brown oil, 60% yield. ^{1}H NMR ($CDCl_3$): δ 1.51−1.53 (m, 2H), 1.84−1.89 (m, 2H), 1.93−1.98 (m, 2H), 2.27 (s, 3H), 2.45−2.50 (m, 6H), 2.69−2.73 (br t, 2H), 2.85 (t, 2H, J = 6.8 Hz), 2.85 (br s, 4H), 3.85 (s, 3H), 3.91 (t, 2H, J = 6.1 Hz), 6.90−6.93 (m, 2H), 7.03−7.06 (m, 2H), 7.21 (dd, 1H, J = 1.5 and 7.3 Hz), 7.25 (td, 1H, J = 1.5 and 7.8 Hz), 7.55−7.58 (m, 2H). ^{13}C NMR (500 MHz, $CDCl_3$): δ 162.6; 158.4; 155.6; 134.5; 133.5; 131.3; 129.8; 129.7; 127.9; 122.6; 118.2; 113.5; 58.13; 55.2; 53.2; 50.6; 42.7; 31.4; 24.1; 22.0; 21.21; 19.25. GC/MS m/z 473 (M^+ + 1, 2), 472 (M^+, 9), 281 (42), 234 (100), 205 (51). Anal. ($C_{29}H_{36}N_4O_2$·2HCl·H_2O) C, H, N.

*7-[2-[4-[2-(4-Methoxyphenyl)phenyl]piperazin-1-yl]ethoxy]-4-methyl-2H-chromen-2-one (**20a**).* Eluted with $CHCl_3$/EtOAc, 1:1. Pale yellow oil, 71% yield. ^{1}H NMR ($CDCl_3$): δ 2.39 (s, 3H), 2.54 (br s, 4H), 2.84 (br t, 2H), 2.91 (br s, 4H), 3.85 (s, 3H), 4.15 (br t, 2H), 6.13 (d, 1H, J = 1.5 Hz), 6.80 (d, 1H, J = 2.5 Hz), 6.86 (dd, 1H, J = 2.5 and 8.8 Hz), 6.92−6.95 (m, 2H), 7.03−7.06 (m, 2H), 7.22 (dd, 1H, J = 1.5 and 7.3 Hz), 7.24−7.27 (m, 1H), 7.48 (d, 1H, J = 8.8 Hz), 7.56−7.59 (m, 2H). ESI-MS m/z 493 (M + Na)$^+$. ESI-MS/MS m/z 493 (89), 295 (100). Anal. ($C_{29}H_{30}N_2O_4$·HCl) C, H, N.

*6-[3-[4-[2-(4-Methoxyphenyl)phenyl]piperazin-1-yl]propoxy]-4-methyl-2H-chromen-2-one (**20b**).* Eluted with CH_2Cl_2/EtOAc, 1:1. Transparent oil, 15% yield. ^{1}H NMR ($CDCl_3$): δ 1.94−1.99 (m, 2H), 2.39 (br s, 7H), 2.50−2.52 (br t, 2H), 2.86 (br s, 4H), 3.85 (s, 3H), 4.03−4.07 (br t, 2H), 6.12 (s, 1H), 6.80−6.85 (m, 2H), 6.91−6.94 (m, 2H), 7.01−7.27 (m, 2H), 7.20−7.27 (m, 3H), 7.47 (d, 1H, J = 8.2 Hz), 7.56−7.59 (m, 2H). ^{13}C NMR (500 MHz, $CDCl_3$): δ 162.2; 161.5; 158.5; 155.4; 152.7; 134.7; 133.7; 131.5; 130.0; 128.1; 125.6; 122.8; 118.3; 113.7; 112.7; 112.0; 101.6; 66.9; 55.4; 55.1; 53.6; 50.9; 26.6; 18.8. ESI-MS m/z 507 (M^+Na)$^+$. ESI-MS/MS m/z 507 (100), 309 (63). Anal. ($C_{30}H_{32}N_2O_4$·HCl) C, H, N.

*7-[4-[4-[2-(4-Methoxyphenyl)phenyl]piperazin-1-yl]butoxy]-4-methyl-2H-1-chromen-2-one (**20c**).* Eluted with $CHCl_3$/MeOH, 98:2. Pale yellow oil, 36% yield. ^{1}H NMR ($CDCl_3$): δ 1.65−1.72 (m, 2H), 1.85−1.94 (m, 2H,) 2.38−2.43 (m + d, 9H, J = 1.1 Hz), 2.85 (app t, 4H), 3.86 (s, 3H), 4.14 (t, 2H, J = 6.0 Hz), 6.17 (d, 1H, J = 1.1 Hz), 6.87−6.95 (m, 3H), 7.00−7.08 (m, 2H), 7.20−7.23 (m, 3H), 7.43 (d, 1H, J = 8.8 Hz), 7.55−7.60 (m, 2H). ESI-MS m/z 497 (M + H)$^+$. ESI-MS/MS m/z 497 (69), 335 (100). Anal. ($C_{31}H_{34}N_2O_4$·HCl·H_2O) C, H, N.

*6-[2-[4-[2-(4-Methoxyphenyl)phenyl]piperazin-1-yl]ethoxy]-2-methyl-2H-benzo[b][1,4]oxazin-3(4H)-one (**26a**).* Eluted with $CHCl_3$/MeOH, 98:2. Transparent oil, 38% yield. ^{1}H NMR ($CDCl_3$): δ 1.55 (d, 3H, J = 6.9 Hz), 2.53 (br s, 4H), 2.79−2.81 (m, 2H), 2.89 (br t, 4 H), 3.86 (s, 3H), 4.04 (app t, 2H), 4.57 (q, 1H, J = 6.9 Hz), 6.36 (d, 1H, J = 2.9 Hz), 6.49 (dd, 1H, J = 2.9 and 8.8 Hz), 6.87 (d, 1H, J = 8.8 Hz), 6.92−6.95 (m, 2H), 7.01−7.07 (m, 2H), 7.21−7.27 (m, 2H), 7.55−7.58 (m, 2H), 8.27 (s, 1H, D_2O exchanged). ESI-MS m/z 474 (M + H)$^+$. ESI-MS/MS m/z 474 (76), 226 (100). Anal. ($C_{28}H_{31}N_3O_4$·2HCl) C, H, N.

*6-[3-[4-[2-(4-Methoxyphenyl)phenyl]piperazin-1-yl]propoxy]-2-methyl-2H-benzo[b][1,4]oxazin-3(4H)-one (**26b**).* Eluted with $CHCl_3$/MeOH, 98:2. Transparent oil, 17% yield. ^{1}H NMR ($CDCl_3$): δ 1.55 (d, 3H, J = 2.5 Hz), 1.92−1.95 (m, 2H), 2.43 (br s, 4H), 2.51 (app t, 2H), 2.88 (br s, 4 H), 3.85 (s, 3H), 3.93 (t, 2H, J = 6.4 Hz), 4.57 (q, 1H, J = 6.9 Hz), 6.34 (d, 1H, J = 2.5 Hz), 6.49 (dd, 1H, J = 2.5 and 8.8 Hz), 6.86 (d, 1H, J = 8.8 Hz), 6.92−6.94 (m, 2H), 7.01−7.07 (m, 2H), 7.21−7.27 (m, 2H), 7.55−7.56 (m, 2H), 8.13 (s, 1H, D_2O exchanged). GC/MS m/z 488 (M^+ + 1, 5), 487 (M^+, 20), 281 (30), 194 (100), 165 (33), 91 (34). Anal. ($C_{29}H_{33}N_3O_4$·2HCl) C, H, N.

*2-[2-[4-[2-(4-Methoxyphenyl)phenyl]piperazin-1-yl]ethyl]-tetrahydro-1H-pyrrolo[1,2-c]imidazole-1,3(2H)-dione (**33a**).* Eluted with $CHCl_3$/EtOAc, 1:1. Transparent oil, 74% yield. ^{1}H NMR ($CDCl_3$): δ 1.64−1.74 (m, 1H), 1.98−2.07 (m, 2H), 2.17−2.25 (m, 1H), 2.40 (br s, 4H), 2.49−2.58 (m, 2H), 2.78 (br s, 4H), 3.19−3.24 (m, 1H), 3.53−3.59 (m, 2H), 3.64−3.69 (m, 1H), 3.85 (s, 3H), 4.05 (t, 1H, J = 8.3 Hz), 6.90−6.93 (m, 2H), 7.04 (td, 1H, J = 1.0 and 7.4 Hz), 7.19−7.25 (m, 2H), 7.54−7.56 (m, 2H). ^{13}C NMR (500 MHz, $CDCl_3$): δ 174.2; 161.1; 158.5; 150.3; 134.7; 133.7; 131.4; 129.9; 127.9; 122.7; 118.3; 63.4; 55.7; 54.9; 53.6; 53.2; 51.1; 45.9; 36.2; 27.8; 27.0. GC/MS m/z 435 (M^+ + 1, 3), 434 (M^+, 13), 281 (100). Anal. ($C_{25}H_{30}N_4O_3$·HCl·H_2O) C, H, N.

*2-[3-[4-[2-(4-Methoxyphenyl)phenyl]piperazin-1-yl]propyl]-tetrahydro-1H-pyrrolo[1,2-c]imidazole-1,3(2H)-dione (**33b**).* Eluted with $CHCl_3$/EtOAc, 1:1. Brown oil, 43% yield. ^{1}H NMR ($CDCl_3$): δ 1.64−1.71 (m, 2H), 1.72−1.82 (m, 2H), 2.02−2.11 (m, 2H), 2.18−2.28 (m, 2H), 2.34−2.38 (m, 5H), 2.85 (br s, 4H), 3.19−3.27 (m, 1H), 3.48−3.52 (m, 2H), 3.62−3.70 (m, 2H), 3.85 (s, 3H), 4.02−4.07 (m, 1H), 6.92 (d, 2H, J = 8.88 Hz), 6.99−7.07 (m, 2H), 7.19−7.27 (m, 2H), 7.55 (d, 2H, J = 8.8 Hz). GC/MS m/z 449 (M^+ + 1, 20), 448 (M^+, 80), 281 (100), 210 (50), 70 (31). Anal. ($C_{26}H_{32}N_4O_3$·HCl·H_2O) C, H, N.

General Procedure for the Preparation of Compounds 29 and 30. A mixture of 1-[2-(4-methoxyphenyl)phenyl]piperazine or 1(2-acetylphenyl)piperazine (1.2 mmol) and the oxirane **28** (1.0 mmol) in ethanol (20 mL) was refluxed for 5 h. After it was cooled, the solvent was removed in vacuo, and the crude residue was chromatographed as detailed below to give desired pure compound.

*6-{(2R)-2-Hydroxy-3-[4-[2-(4-methoxyphenyl)phenyl]piperazin-1-yl]propoxy}-2-methyl-2H-benzo[b][1,4]oxazin-3(4H)-one (**29**).* Eluted with $CHCl_3$/AcOEt, 1:1. White semisolid, 30% yield. ^{1}H NMR ($CDCl_3$): δ 1.62 (br s, 1H, D_2O exchanged), 1.47 (d, 3H, J = 6.8 Hz), 2.30−2.32 (m, 2H,), 2.39−2.45 (m, 2H), 2.48−2.54 (m, 2H), 2.79−2.83 (m, 4H), 3.78 (s, 3H), 3.82 (d, 2H, J = 4.9 Hz), 3.94−3.97 (m, 1H), 4.49 (q, 1H, J = 6.8 Hz), 6.79 (d, 1H, J = 8.8 Hz), 6.84−6.87 (m, 2H), 6.94 (dd, 1H, J = 1.1 and 8.3 Hz), 6.99 (td, 1H, J = 1.5 and 7.3 Hz), 7.14−7.20 (m, 4H), 7.48−7.51 (m, 2H), 8.35 (br, 1H, D2O exchanged). ^{13}C NMR (500 MHz, $CDCl_3$): δ 168.0; 167.9; 158.7; 153.4; 147.8; 137.6; 137.5; 134.9; 132.6; 131.5; 129.8; 128.2; 127.5; 124.2; 118.7; 117.2; 114.0; 109.9; 102.6; 73.2; 70.4; 64.6; 61.0; 55.4; 54.7; 53.4; 47.8; 47.7; 16.0. ESI-MS m/z 526 (M^+Na)$^+$. ESI-MS/MS m/z 526 (100), 347 (11). Anal. ($C_{29}H_{33}N_3O_5$·HCl) C, H, N.

*6-[3-[4-(2-Acetylphenyl)piperazin-1-yl]-(2R)-2-hydroxypropoxy]-2-methyl-2H-benzo[b][1,4]oxazin-3(4H)-one (**30**).* Eluted with $CHCl_3$/MeOH, 95:5. Brown oil, 54% yield. ^{1}H NMR ($CDCl_3$): δ 1.50 (d, 3H, J = 6.9 Hz), 1.81 (br s, 1H, D_2O exchanged), 2.56−2.64 (m, 4H), 2.65 (s, 3H), 2.78−2.83 (m, 2H), 3.05 (br, 4 H), 3.94−3.96 (m, 2H), 4.09−4.11 (m, 1H), 4.57 (q, 1H, 6.9 Hz), 6.44 (s, 1H), 6.52 (dd, 1H, J = 2.4 and 8.8 Hz), 6.87 (d, 1H, J = 8.8 Hz), 7.05−7.08 (m, 2H), 7.39−7.42 (m, 2H), 8.49 (br s, 1H, D_2O exchanged). ESI-MS m/z 462 (M + Na)$^+$. ESI-MS/MS m/z 462 (100). Anal. ($C_{24}H_{29}N_3O_5$·2HCl) C, H, N.

Radioligand Binding Assays. *Materials.* Cell culture reagents were purchased from EuroClone (Milan, Italy). G418 (Geneticin), 5-HT, and NAN-190 were obtained from Sigma-Aldrich (Milano, Italy). 5-CT was purchased from Tocris Bioscience (Bristol, UK). [^{3}H]-5-CT and [^{3}H]-8-OH-DPAT were obtained from PerkinElmer Life and Analytical Sciences (Boston, MA, USA). MultiScreen plates with Glass fiber filters was purchased from Merck Millipore (Billerica, MA, USA). pcDNA3.1(+) vector containing the target 5-HT_{1A} DNA sequence was purchased from cDNA Resource Center (Bloomsberg, PA, USA), and FuGENE HD Transfection Reagent was obtained from Promega (Madison, Wisconsin, USA).

Cell Culture. HEK-293 cell line was grown in DMEM high glucose supplemented with 10% fetal bovine serum, 2 mM glutamine, 100 U/mL penicillin, and 100 μg/mL streptomycin, in a humidified incubator at 37 °C with a 5% CO_2 atmosphere. HEK-293-5-HT_{7A} and HEK-293-5-HT_{1A} transfected cell lines were grown in DMEM high glucose supplemented with 10% fetal bovine serum, 2 mM glutamine, 100 U/

https://doi.org/10.1021/acschemneuro.0c00647
ACS Chem. Neurosci. 2021, 12, 1313−1327

mL penicillin, 100 μg/mL streptomycin, and 0.8 μg/mL G418, in a humidified incubator at 37 °C with a 5% CO_2 atmosphere.

Radioligand Binding at Human Cloned 5-HT$_7$Rs. 5-HT$_7$R binding was carried out as previously reported.[57] The experiment was performed in MultiScreen plates (Merck Millipore) with Glass fiber filters (GF/C), presoaked in 0.3% PEI for 20 min. After this time, 130 μg of HEK-293-5-HT$_{7A}$ membranes, 1 nM [^{3}H]-5-CT, and the test compounds were suspended in 0.25 mL of incubation buffer (50 mM Tris−HCl, pH 7.4, 4 mM $MgCl_2$, 0.1% ascorbic acid, 10 μM pargyline hydrochloride). The samples were incubated for 60 min at 37 °C. The incubation was stopped by rapid filtration, and the filters were washed with 3 × 0.25 mL of ice-cold buffer (50 mM TRIS-HCl, pH 7.4). Nonspecific binding was determined in the presence of 10 μM 5-CT. Approximately 90% of specific binding was determined under these conditions. Concentrations required to inhibit 50% of radioligand specific binding (IC_{50}) were determined by using six to nine different concentrations of the drug studied in two or three experiments with samples in duplicate. Apparent inhibition constants (K_i) values were determined by nonlinear curve fitting, using the Prism, version 5.0, GraphPad software.

Radioligand Binding at Human Cloned 5-HT$_{1A}$R. 5-HT$_{1A}$R binding was carried out as already reported.[57] The experiment was performed in MultiScreen plates (Merck Millipore) with Glass fiber filters (GF/C), presoaked in 0.3% PEI for 20 min. After this time, 100 μg of HEK-293-5-HT$_{1A}$ membranes, 1.5 nM [^{3}H]-8-OH-DPAT, and the test compound were suspended in a 0.25 mL of incubation buffer (50 mM Tris−HCl pH 7.4, 4 mM $MgCl_2$, 0.1% ascorbic acid, 0.1 nM EDTA, 10 μM pargyline hydrochloride). The samples were incubated for 60 min at 25 °C. The incubation was stopped by rapid filtration, and the filters were washed with 3 × 0.25 mL of ice-cold buffer (50 mM TRIS-HCl, pH 7.4). Nonspecific binding was determined in the presence of 10 μM NAN-190. Approximately 90% of specific binding was determined under these conditions. Concentrations required to inhibit 50% of radioligand specific binding (IC_{50}) were determined by using six to nine different concentrations of the test compound in two or three experiments with samples in duplicate. Apparent inhibition constants (K_i) values were determined by nonlinear curve fitting, using the Prism, version 5.0, GraphPad software.

Radioligand Binding at Human Cloned Dopamine D$_2$ and Serotonin 5-HT$_{2A}$ Receptors. The affinity of the compounds for dopamine D_2 and serotonin 5-HT$_{2A}$ receptors was evaluated in membrane preparations from CHO-K1 cells stably expressing the human cloned D_{2S} receptor or the human cloned 5-HT$_{2A}$ receptor, following previously described procedures.[58] Competition binding experiments were performed using [^{3}H]spiperone (0.2 nM; D_2 receptor) or [^{3}H]ketanserin (1 nM; 5-HT$_{2A}$R) as radioligands. Nonspecific binding was assessed in the presence of 10 μM sulpiride (D_2 receptor) or 1 μM methysergide (5-HT$_{2A}$R). Haloperidol (D_2 receptor) and risperidone (5-HT$_{2A}$R) were included in the assays as reference compounds. Competition binding curves constructed with 6 different concentrations of the compounds were fitted to a one-site competition model using Prism 6 software (GraphPad, San Diego, CA, USA), and equilibrium dissociation constant (K_i) of the compounds was calculated according to the Cheng−Prusoff equation.

Analysis of the cAMP Response Using FRET-Based Biosensor CEPAC. Mouse neuroblastoma N1E115 cells (American Type Culture Collection, Manassas, USA) were seeded onto 18 mm glass coverslips and grown in DMEM containing 10% fetal bovine serum and 1% penicillin/streptomycin at 37 °C in a humidified atmosphere with 5% CO_2. Expression of the cAMP-biosensor CEPAC, 5-HT$_7$R, or 5-HT$_{1A}$R was ensured by transfection (plasmid DNA to biosensor and receptor ratio of 7:3) using Lipofectamine 2000 (Life Technologies). One day after transfection, changes in cAMP levels upon perfusion with 10 μM **8c**, **20b**, **29**, LP-211, or 5-CT 5-HT$_7$R in Tyrode's buffer (150 mM NaCl; 5 mM KCl; 1 mM $MgCl_2$; 2 mM $CaCl_2$; 10 mM HEPES; pH 7.4; adjusted osmolarity) were monitored in real-time under a Zeiss LSM 780 confocal laser-scanning microscope. A 61 cycle time series with a 10 s interval was recorded in online fingerprinting mode of the ZEN acquisition software with the following settings: image dimension = 1024 pixels × 1024 pixels, resolution = 0.346 μm × 0.346 μm, excitation = 440 nm diode and 561 nm DPSS laser lines, filters = MBS 445, MBS 458/561, objective = C-Apochromat 40×/1.2W Corr. Corresponding reference spectra for the online fingerprinting mode were obtained from separate measurements with a single fluorophore transfection. The semiautomatic biosensor data analysis relied on custom-written MATLAB scripts comprising data import, preprocessing, shift correction in the *xy*-plane for each time point, the exclusion of saturated pixels from evaluation, background correction, and faint data blurring with a kernel size of 0.5 according to Pawley.[59] The pixel-based ratio was calculated for selected regions of interest (ROIs) for evaluation. Traces were normalized according to their mean ratio before stimulation.

Functional Assays at 5-HT$_{2A}$ Receptor. The efficacy of compounds **8c**, **20b**, and **29** at 5-HT$_{2A}$ receptor was investigated in assays of inositol phosphate (IP) production in the CHO-K1 cell line stably expressing the cloned human 5-HT$_{2A}$ receptor employed in radioligand binding assays. Cellular IP levels were quantified by using the homogeneous time-resolved fluorescence (HTRF)-based inositol monophosphate kit IP-One Gq kit (Cisbio, Bioassays, Codolet, France) following the manufacturer protocol. Cells were seeded in 96-well plates in culture medium DMEM (Gibco, ThermoFisher Scientific, Madrid, Spain) supplemented with 10% (v/v) dialyzed fetal bovine serum (Sigma-Aldrich, Madrid, Spain), 100 U/mL penicillin/0.1 mg/mL streptomycin (Sigma-Aldrich, Madrid, Spain), and 2 mM L-glutamine (Sigma-Aldrich, Madrid, Spain)) and maintained during 24 h at 37 °C in a 5% CO_2 humidified atmosphere. Prior to the assay, cell supernatant was removed and for assessment of possible agonist effect, and cells were incubated with the compounds (0.1 nM−100 μM) or 5-HT (0.1 nM−100 μM) as control agonist in stimulation buffer for 20 min at 37 °C. After this time, IP levels were quantified. For assessment of possible antagonist effect, the compounds (0.1 nM−100 μM) were added to the cells 10 min prior to the addition of 1 μM 5-HT, and assays were subsequently carried out as described above. Risperidone (0.1 nM−100 μM) was used as control antagonist in these assays. In all cases, basal IP levels were determined in control wells in the absence of compound and agonist. Antagonist concentration−response curves were fitted to a sigmoidal dose−response (inhibition) model (Hill slope (nH) = 1, with best fit in comparison to sigmoidal dose−response (variable slope) model, $P < 0.05$, extra sum-of-squares F test) using Prism 6 software (GraphPad, San Diego, CA) to retrieve pIC_{50} (−log IC_{50}) values.

Stability Assays in Rat Liver Microsomes. Test compounds were preincubated at 37 °C with rat liver microsomes (Tebu-Bio, Milan, Italy) (1.0 mg/mL microsomal protein) at 10 μM final concentration in 100 mM potassium phosphate buffer (pH 7.4) for 10 min. Metabolic reactions were initiated by the addition of the NADPH regenerating system (containing 10 mM NADP, 50 mM glucose-6-phosphate, and 10 unit/mL glucose-6-phosphate dehydrogenase, final glucose-6-phosphate dehydrogenase concentration, 1 unit/mL). Aliquots were removed at specific time end points and immediately mixed with an equal volume of cold acetonitrile containing the internal standard. To assess in vitro in vitro half-life ($t_{1/2}$) the aliquots were removed at 0, 5, 15, 30, 60, and 120 min. Test compound incubated with microsomes without NADPH regenerating system was included. Quenched samples were centrifuged at 4500 rpm for 15 min, and the supernatants were injected for quantification analysis. Samples (100 μL) were analyzed by using an Agilent 1260 Infinity Binary LC System equipped with a diode array detector (Open Lab software was used to analyze the chromatographic data) and a Phenomenex Gemini C-18 column (250 mm × 4.6 mm, 5 μm particle size). The samples were eluted using CH_3CN/20 mM ammonium formate pH 5.5 (70:30, v/v) as eluent (1 mL/min). Concentrations were quantified by measuring the area under the peak. The percentage of the parent compound remaining after a 30 min incubation has been calculated according to the equation

$$\%\text{of parent compound remaining after 30 min} = C_{\text{parent}}/C_{\text{control}} \times 100$$

https://doi.org/10.1021/acschemneuro.0c00647
ACS Chem. Neurosci. 2021, 12, 1313−1327

where C_{parent} is ligand concentration after incubation with microsome fraction and NADPH regenerating system and $C_{control}$ is ligand concentration after incubation with microsome fraction only.

The in vitro half-life ($t_{1/2}$) was calculated using the expression $t_{1/2} = 0.693/b$, where b is the slope found in the linear fit of the natural logarithm of the fraction remaining of the parent compound vs incubation time.[41] In vitro half-life was then used to calculate the intrinsic plasma clearance (CL_{int}) according to the following equation:

$$CL_{int} = \frac{0.693}{\text{in vitro } t_{1/2}} \times \frac{1}{\text{mg/mL microsomal protein}}$$

Internal positive controls were aripiprazole (C_{int} = 6.93 mL/mg/min, $t_{1/2}$ = 100 min) and LP-211 (C_{int}= 45.9 mL/mg/min, $t_{1/2}$ = 45.9 min).

■ ASSOCIATED CONTENT

Supporting Information

The Supporting Information is available free of charge at https://pubs.acs.org/doi/10.1021/acschemneuro.0c00647.

General procedures and spectroscopic data of intermediates **7a,b**, **12**, **13**, **15**, **16**, **19a−c**, **22**, **23**, **24**, **25a,b**, **26b**, **28**, and **32a,b**; formula, molecular weight, and monoisotopic mass of the synthesized compounds; elemental analysis of target compounds; off-target affinities of selected target compounds; and ^{1}H NMR spectra of target compounds **8a−c**, **9**, **14a,b**, **20a−c**, **26a−c**, **33a,b**, **29**, and **30** (PDF)

■ AUTHOR INFORMATION

Corresponding Authors

Enza Lacivita − *Dipartimento di Farmacia−Scienze del Farmaco, Università degli Studi di Bari Aldo Moro, 70125 Bari, Italy*; orcid.org/0000-0003-2443-1174; Email: enza.lacivita@uniba.it

Marcello Leopoldo − *Dipartimento di Farmacia−Scienze del Farmaco, Università degli Studi di Bari Aldo Moro, 70125 Bari, Italy*; orcid.org/0000-0001-8401-2815; Email: marcello.leopoldo@uniba.it

Authors

Mauro Niso − *Dipartimento di Farmacia−Scienze del Farmaco, Università degli Studi di Bari Aldo Moro, 70125 Bari, Italy*

Margherita Mastromarino − *Dipartimento di Farmacia−Scienze del Farmaco, Università degli Studi di Bari Aldo Moro, 70125 Bari, Italy*

Andrea Garcia Silva − *Center for Research in Molecular Medicine and Chronic Diseases (CIMUS), Universidade de Santiago de Compostela, 15782 Santiago de Compostela, Spain*

Cibell Resch − *Cellular Neurophysiology, Hannover Medical School, 30625 Hannover, Germany*

Andre Zeug − *Cellular Neurophysiology, Hannover Medical School, 30625 Hannover, Germany*

María I. Loza − *Center for Research in Molecular Medicine and Chronic Diseases (CIMUS), Universidade de Santiago de Compostela, 15782 Santiago de Compostela, Spain*

Marián Castro − *Center for Research in Molecular Medicine and Chronic Diseases (CIMUS), Universidade de Santiago de Compostela, 15782 Santiago de Compostela, Spain*

Evgeni Ponimaskin − *Cellular Neurophysiology, Hannover Medical School, 30625 Hannover, Germany*

Complete contact information is available at: https://pubs.acs.org/10.1021/acschemneuro.0c00647

Author Contributions

The manuscript was written through contributions of all authors. All authors have given approval to the final version of the manuscript.

Funding

The present work was partially supported by Telethon Foundation Grant GGP13145 (M.L.) and by German Research Foundation (DFG) (grant number PO732 to E.P. and grant number ZE994/2 to A.Z.). A.G.S., M.I.L., and M.C. acknowledge support from the Spanish Ministry of Economy and Competitiveness (MINECO) (grant number SAF2014-57138-C2−1-R), Xunta de Galicia (Centro singular de investigación de Galicia accreditation 2019−2022, grant number ED431G 2019/02), and the European Union (European Regional Development Fund - ERDF). COST Action CA 18133 "European Research Network on Signal Transduction − ERNEST" is gratefully acknowledged. Funding for open access charge: COST Action CA18133 (ERNEST).

Notes

The authors declare no competing financial interest.

■ ABBREVIATIONS

5-HT, serotonin; 5-HT_{1A}R, serotonin 1A receptor; 5-HT_{2A}R, serotonin 2A receptor; 5-HT_7R, serotonin 7 receptor; 8-OH-DPAT, 8-hydroxy-2-dipropylaminotetralin; (+)-5-FTP, (+)-5-(2′-fluorophenyl)-*N*,*N*-dimethyl-1,2,3,4-tetrahidronaphthalen-2-amine; ADME, absorption, distribution, metabolism, and excretion; ASD, autism spectrum disorder; cAMP, cyclic adenosine monophosphate; $CL_{int\ app}$, apparent intrinsic clearance; CNS, central nervous system; FRET, fluorescence resonance energy transfer; SAR, structure−activity relationship; SSRI, selective serotonin reuptake inhibitor

■ REFERENCES

(1) American Psychiatric Association. (2013) *Diagnostic and Statistical Manual of Mental Disorders*, 5th ed., American Psychiatric Publishing, Washington DC.

(2) https://www.cdc.gov/ncbddd/autism/addm-community-report/executive-summary.html (accessed on March 2021).

(3) Lacivita, E., Perrone, R., Margari, L., and Leopoldo, M. (2017) Targets for Drug Therapy for Autism Spectrum Disorder: Challenges and Future Directions. *J. Med. Chem. 60*, 9114−9141.

(4) Whitaker-Azmitia, P. (2001) Serotonin and brain development: role in human developmental diseases. *Brain Res. Bull. 56*, 479−485.

(5) Wirth, A., Holst, K., and Ponimaskin, E. (2017) How serotonin receptors regulate morphogenic signalling in neurons. *Prog. Neurobiol. 151*, 35−56.

(6) Muller, C. L., Anacker, A. M. J., and Veenstra-VanderWeele, J. (2016) The serotonin system in autism spectrum disorder: From biomarker to animal models. *Neuroscience 321*, 24−41.

(7) Chaliha, D., Albrecht, M., Vaccarezza, M., Takechi, R., Lam, V., Al-Salami, H., and Mamo, J. A. (2020) Systematic review of the valproic-acid-induced rodent model of autism. *Dev. Neurosci. 42*, 12−48.

(8) Kinast, K., Peeters, D., Kolk, S. M., Schubert, D., and Homberg, J. R. (2013) Genetic and pharmacological manipulations of the serotonergic system in early life: neurodevelopmental underpinnings of autism-related behavior. *Front. Cell. Neurosci. 7*, 72.

(9) Guo, Y.-P., and Commons, K. G. (2017) Serotonin neurons abnormalities in the BTBR mouse model of autism. *Autism Res. 10*, 66−77.

(10) Brandenburg, C., and Blatt, G. J. (2019) Differential serotonin transporter (5-HTT) and 5-HT2 receptor density in limbic and neocortical areas of adults and children with autism spectrum disorders: implications for selective serotonin reuptake inhibitor efficacy. *J. Neurochem. 151*, 642−655.

(11) Chugani, D. C., Chugani, H. T., Wiznitzer, M., Parikh, S., Evans, P. A., Hansen, R. L., Nass, R., Janisse, J. J., Dixon-Thomas, P., Behen, M., et al. (2016) Efficacy of Low-Dose Buspirone for Restricted and Repetitive Behavior in Young Children with Autism Spectrum Disorder: A Randomized Trial. *J. Pediatr. 170*, 45−53.
(12) Gould, G. G., Hensler, J. G., Burke, T. F., Benno, R. H., Onaivi, E. S., and Daws, L. C. (2011) Density and function of central serotonin (5-HT) transporters, 5-HT_{1A} and 5-HT_{2A} receptors, and effects of their targeting on BTBR T+tf/J mouse social behavior. *J. Neurochem. 116*, 291−303.
(13) Wang, C.-C., Lin, H.-C., Chan, Y.-H., Gean, P.-W., Yang, Y. K., and Chen, P. S. (2013) 5-HT1A-receptor agonist modified amygdala activity and amygdala-associated social behavior in a valproate-induced rat autism model. *Int. J. Neuropsychopharmacol. 16*, 2027−2039.
(14) Amodeo, D. A., Rivera, E., Dunn, J. T., and Ragozzino, M. E. (2016) M100907 attenuates elevated grooming behavior in the BTBR mouse. *Behav. Brain Res. 313*, 67−70.
(15) Amodeo, D. A., Rivera, E., Cook, E. H., Sweeney, J. A., and Ragozzino, M. E. (2017) 5-HT_{2A} receptor blockade in dorsomedial striatum reduces repetitive behaviors in BTBR mice. *Genes Brain. Behav. 16*, 342−351.
(16) de Bruin, N. M. W. J., van Loevezijn, A., Wicke, K. M., de Haan, M., Venhorst, J., Lange, J. H. M., de Groote, L., van der Neut, M. A. W., Prickaerts, J., Andriambeloson, E., et al. (2016) G. The selective 5-HT_6 receptor antagonist SLV has putative cognitive- and social interaction enhancing properties in rodent models of cognitive impairment. *Neurobiol. Learn. Mem. 133*, 100−117.
(17) Costa, L., Spatuzza, M., D'Antoni, S., Bonaccorso, C. M., Trovato, C., Musumeci, S. A., Leopoldo, M., Lacivita, E., Catania, M. V., and Ciranna, L. (2012) Activation of 5-HT_7 serotonin receptors reverses metabotropic glutamate receptor-mediated synaptic plasticity in wild-type and Fmr1 knockout mice, a model of Fragile X syndrome. *Biol. Psychiatry 72*, 924−933.
(18) Costa, L., Sardone, L. M., Lacivita, E., Leopoldo, M., and Ciranna, L. (2015) Novel agonists for serotonin 5-HT_7 receptors reverse metabotropic glutamate receptor-mediated long-term depression in the hippocampus of wild-type and Fmr1 KO mice, a model of Fragile X Syndrome. *Front. Behav. Neurosci. 9*, 65.
(19) Costa, L., Sardone, L. M., Bonaccorso, C. M., D'Antoni, S., Spatuzza, M., Gulisano, W., Tropea, M. R., Puzzo, D., Leopoldo, M., Lacivita, E., Catania, M. V., Ciranna, L., et al. (2018) Activation of serotonin 5-HT_7 receptors modulates hippocampal synaptic plasticity by stimulation of adenylate cyclases and rescues learning and behavior in a mouse model of fragile X syndrome. *Front. Mol. Neurosci. 11*, 353.
(20) De Filippis, B., Nativio, P., Fabbri, A., Ricceri, L., Adriani, W., Lacivita, E., Leopoldo, M., Passarelli, F., Fuso, A., and Laviola, G. (2014) Pharmacological stimulation of the brain serotonin receptor 7 as a novel therapeutic approach for Rett syndrome. *Neuropsychopharmacology 39*, 2506−2518.
(21) De Filippis, B., Chiodi, V., Adriani, W., Lacivita, E., Mallozzi, C., Leopoldo, M., Domenici, M. R., Fuso, A., and Laviola, G. (2015) Long-lasting beneficial effects of central serotonin receptor 7 stimulation in female mice modeling Rett syndrome. *Front. Behav. Neurosci. 9*, 86.
(22) Valenti, D., de Bari, L., Vigli, D., Lacivita, E., Leopoldo, M., Laviola, G., Vacca, R. A., and De Filippis, B. (2017) Stimulation of the brain serotonin receptor 7 rescues mitochondrial dysfunction in female mice from two models of Rett syndrome. *Neuropharmacology 121*, 79−88.
(23) Vigli, D., Rusconi, L., Valenti, D., La Montanara, P., Cosentino, L., Lacivita, E., Leopoldo, M., Amendola, E., Gross, C., Landsberger, N., et al. (2019) Rescue of prepulse inhibition deficit and brain mitochondrial dysfunction by pharmacological stimulation of the central serotonin receptor 7 in a mouse model of CDKL5 Deficiency Disorder. *Neuropharmacology 144*, 104−114.
(24) Kroeze, W. K., Hufeisen, S. J., Popadak, B. A., Renock, S. M., Steinberg, S., Ernsberger, P., Jayathilake, K., Meltzer, H. Y., and Roth, B. L. (2003) H1-histamine receptor affinity predicts short-term weight gain for typical and atypical antipsychotic drugs. *Neuropsychopharmacology 28*, 519−526.
(25) Witt, N. A., Lee, B., Ghent, K., Zhang, W. Q., Pehrson, A. L., Sánchez, C., and Gould, G. G. (2019) Vortioxetine reduces marble burying but only transiently enhances social interaction preference in adult male BTBR T+Itpr3tf/J mice. *ACS Chem. Neurosci. 10*, 4319−4327.
(26) Canal, C. E., Felsing, D. E., Liu, Y., Zhu, W., Wood, J. T., Perry, C. K., Vemula, R., and Booth, R. G. (2015) An orally active phenylaminotetralin-chemotype serotonin 5-HT_7 and 5-HT_{1A} receptor partial agonist that corrects motor stereotypy in mouse models. *ACS Chem. Neurosci. 6*, 1259−1270.
(27) Armstrong, J. L., Casey, A. B., Saraf, T. S., Mukherjee, M., Booth, R. G., and Canal, C. E. (2020) (S)-5-(2′-Fluorophenyl)-N,N-dimethyl-1,2,3,4-tetrahydronaphthalen-2-amine, a serotonin receptor modulator, possesses anticonvulsant, prosocial, and anxiolytic-like properties in an Fmr1 knockout mouse model of fragile X syndrome and autism spectrum disorder. *ACS Pharmacol. Transl. Sci. 3*, 509−523.
(28) Hedlund, P. B., Leopoldo, M., Caccia, S., Sarkisyan, G., Fracasso, C., Martelli, G., Lacivita, E., Berardi, F., and Perrone, R. (2010) LP-211 is a brain penetrant selective agonist for the serotonin 5-HT7 receptor. *Neurosci. Lett. 481*, 12−16.
(29) Leopoldo, M., Lacivita, E., Contino, M., Colabufo, N. A., Berardi, F., and Perrone, R. (2007) Structure-activity relationship study on N-(1,2,3,4-tetrahydronaphthalen-1-yl)-4-aryl-1-piperazinehexanamides, a class of 5-HT_7 receptor agents. 2. *J. Med. Chem. 50*, 4214−4221.
(30) Salerno, L., Pittalà, V., Modica, M. N., Siracusa, M. A., Intagliata, S., Cagnotto, A., Salmona, M., Kurczab, R., Bojarski, A. J., and Romeo, G. (2014) Structure-activity relationships and molecular modeling studies of novel arylpiperazinylalkyl 2-benzoxazolones and 2-benzothiazolones as 5-HT7 and 5-HT1A receptor ligands. *Eur. J. Med. Chem. 85*, 716−726.
(31) Zajdel, P., Kos, T., Marciniec, K., Satała, G., Canale, V., Kamiński, K., Hołuj, M., Lenda, T., Koralewski, R., Bednarski, M., et al. (2018) Novel multi-target azinesulfonamides of cyclic amine derivatives as potential antipsychotics with pro-social and pro-cognitive effects. *Eur. J. Med. Chem. 145*, 790−804.
(32) Lacivita, E., Podlewska, S., Speranza, L., Niso, M., Satała, G., Perrone, R., Perrone-Capano, C., Bojarski, A. J., and Leopoldo, M. (2016) Structural modifications of the serotonin 5-HT_7 receptor agonist N-(4-cyanophenylmethyl)-4-(2-biphenyl)-1-piperazinehexanamide (LP-211) to improve in vitro microsomal stability: a case study. *Eur. J. Med. Chem. 120*, 363−379.
(33) Forster, E. A., Cliffe, I. A., Bill, D. J., Dover, G. M., Jones, D., Reilly, Y., and Fletcher, A. (1995) A pharmacological profile of the selective silent 5-HT1A receptor antagonist, WAY-100635. *Eur. J. Pharmacol. 281*, 81−88.
(34) Bojarski, A. J., Paluchowska, M. H., Duszyńska, B., Bugno, R., Kłodzińska, A., Tatarczyńska, E., and Chojnacka-Wójcik, E. (2006) Structure-intrinsic activity relationship studies in the group of 1-imido/amido substituted 4-(4-arylpiperazin-1-yl)cyclohexane derivatives; new, potent 5-HT_{1A} receptor agents with anxiolytic- like activity. *Bioorg. Med. Chem. 14*, 1391−1402.
(35) Kumar, J. S., Prabhakaran, J., Majo, V. J., Milak, M. S., Hsiung, S. C., Tamir, H., Simpson, N. R., Van Heertum, R. L., Mann, J. J., and Parsey, R. V. (2007) Synthesis and in vivo evaluation of a novel 5-HT_{1A} receptor agonist radioligand (O-methyl- ^{11}C]2-(4-(4-(2-methoxyphenyl)piperazin-1-yl)butyl)-4-methyl-1,2,4-triazine-3,5-(2H,4H)dione in nonhuman primates. *Eur. J. Nucl. Med. Mol. Imaging 34*, 1050−1060.
(36) López-Rodríguez, M. L., Morcillo, M. J., Fernández, E., Benhamú, B., Tejada, I., Ayala, D., Viso, A., Campillo, M., Pardo, L., Delgado, M., et al. (2005) Synthesis and structure-activity relationships of a new model of arylpiperazines. 8. Computational simulation of ligand-receptor interaction of 5-HT1AR agonists with selectivity over alpha1-adrenoceptors. *J. Med. Chem. 48*, 2548−2558.
(37) Cantillon, M., Prakash, A., Alexander, A., Ings, R., Sweitzer, D., and Bhat, L. (2017) Dopamine serotonin stabilizer RP5063: a randomized, double-blind, placebo-controlled multicenter trial of safety and efficacy in exacerbation of schizophrenia or schizoaffective disorder. *Schizophr. Res. 189*, 126−133.

https://doi.org/10.1021/acschemneuro.0c00647
ACS Chem. Neurosci. 2021, 12, 1313−1327

(38) Chen, Y., Wang, S., Xu, X., Liu, X., Yu, M., Zhao, S., Liu, S., Qiu, Y., Zhang, T., Liu, B. F., et al. (2013) Synthesis and biological investigation of coumarin piperazine (piperidine) derivatives as potential multireceptor atypical antipsychotics. *J. Med. Chem. 56*, 4671−4690.
(39) Bojarski, A. J. (2006) Pharmacophore models for metabotropic 5-HT receptor ligands. *Curr. Top. Med. Chem. 6*, 2005−2026.
(40) Wager, T. T., Hou, X., Verhoest, P. R., and Villalobos, A. (2016) Central Nervous System Multiparameter Optimization Desirability: application in drug discovery. *ACS Chem. Neurosci. 7*, 767−775.
(41) Obach, R. S., Baxter, J. G., Liston, T. E., Silber, B. M., Jones, B. C., MacIntyre, F., Rance, D. J., and Wastall, P. (1997) The prediction of human pharmacokinetic parameters from preclinical and in vitro metabolism data. *J. Pharmacol. Exp. Ther. 283*, 46−58.
(42) Kumar, J. S., Majo, V. J., Hsiung, S. C., Millak, M. S., Liu, K. P., Tamir, H., Prabhakaran, J., Simpson, N. R., Van Heertum, R. L., Mann, J. J., et al. (2006) Synthesis and in vivo validation of [O-methyl-11C]2-{4-[4-(7-methoxynaphthalen-1-yl)piperazin-1-yl]butyl}-4-methyl-2H-[1,2,4]triazine-3,5-dione: a novel 5-HT_{1A} receptor agonist positron emission tomography ligand. *J. Med. Chem. 49*, 125−134.
(43) Srinivasa, R. G., Prasanna, K. B. N., Manjunatha, S. G., and Kulkarni, A. K. (2005) Process for the preparation of risperidone, WO2005030772.
(44) Lacivita, E., Patarnello, D., Stroth, N., Caroli, A., Niso, M., Contino, M., De Giorgio, P., Di Pilato, P., Colabufo, N. A., Berardi, F., et al. (2012) Investigations on the 1-(2-biphenyl)piperazine motif: identification of new potent and selective ligands for the serotonin7 (5-HT7) receptor with agonist or antagonist action in vitro or ex vivo. *J. Med. Chem. 55*, 6375−6380.
(45) Elgogary, S. R., Hashem, N. M., and Khodeir, M. N. (2015) Synthesis and photooxygenation of linear and angular furocoumarin derivatives as a hydroxyl radical source: psoralen, pseudopsoralen, isopseudopsoralen, and allopsoralen. *J. Heteroc. Chem. 52*, 506−512.
(46) Holloway, B. R., Howe, R., Rao, B. S., and Stribling, D. (1990) Amide derivatives, US4927836.
(47) Pendin, D., Norante, R., De Nadai, A., Gherardi, G., Vajente, N., Basso, E., Kaludercic, N., Mammucari, C., Paradisi, C., Pozzan, T., et al. (2019) A synthetic fluorescent mitochondria-targeted sensor for ratiometric imaging of calcium in live cells. *Angew. Chem., Int. Ed. 58*, 9917−9922.
(48) Brown, J. W., Gangloff, A. R., Jennings, A. J., and Vu, P. H. (2010) Poly (ADP-Ribose) Polymerase (PARP) inhibitors, WO2010111626.
(49) Kolyasnikova, K. N., Vichuzhanin, M. V., Konstantinopol'skii, M. A., Trofimov, S. S., and Gudasheva, T. A. (2012) Synthesis and pharmacological activity of analogs of the endogenous neuropeptide cycloprolylglycine. *Pharm. Chem. J. 46*, 96−102.
(50) Kaar, S. J., Natesan, S., McCutcheon, R., and Howes, O. D. (2020) Antipsychotics: mechanisms underlying clinical response and side-effects and novel treatment approaches based on pathophysiology. *Neuropharmacology 172*, 107704.
(51) Lacivita, E., Niso, M., Stama, M. L., Arzuaga, A., Altamura, C., Costa, L., Desaphy, J. F., Ragozzino, M. E., Ciranna, L., and Leopoldo, M. (2020) Privileged scaffold-based design to identify a novel drug-like 5-HT_7 receptor-preferring agonist to target fragile X syndrome. *Eur. J. Med. Chem. 199*, 112395.
(52) Di, L., Kerns, E. H., Ma, X. J., Huang, Y., and Carter, G. T. (2008) Applications of high throughput microsomal stability assay in drug discovery. *Comb. Chem. High Throughput Screening 11*, 469−476.
(53) Guscott, M. R., Egan, E., Cook, G. P., Stanton, J. A., Beer, M. S., Rosahl, T. W., Hartmann, S., Kulagowski, J., McAllister, G., Fone, K. F. C., et al. (2003) The hypothermic effect of 5-CT in mice is mediated through the 5-HT7 receptor. *Neuropharmacology 44*, 1031−1037.
(54) Salonikidis, P. S., Zeug, A., Kobe, F., Ponimaskin, E., and Richter, D. W. (2008) Quantitative measurement of cAMP concentration using an exchange protein directly activated by a cAMP- based FRET-sensor. *Biophys. J. 95*, 5412−5423.
(55) Prasad, S., Ponimaskin, E., and Zeug, A. (2019) Serotonin receptor oligomerization regulates cAMP-based signaling. *J. Cell. Sci. 132*, 1 DOI: 10.1242/jcs.230334.
(56) Tran, J. A., Pontillo, J., Arellano, M., White, N. S., Fleck, B. A., Marinkovic, D., Tucci, F. C., Lanier, M., Nelson, J., Saunders, J., Foster, A. C., and Chen, C. (2005) Identification of agonists and antagonists of the human melanocortin-4 receptor from piperazinebenzylamines. *Bioorg. Med. Chem. Lett. 15*, 833−837.
(57) Lacivita, E., Niso, M., Hansen, H. D., Di Pilato, P., Herth, M. M., Lehel, S., Ettrup, A., Montenegro, L., Perrone, R., Berardi, F., et al. (2014) Design, synthesis, radiolabeling and in vivo evaluation of potential positron emission tomography (PET) radioligands for brain imaging of the 5-HT_7 receptor. *Bioorg. Med. Chem. 22*, 1736−1750.
(58) Kaczor, A. A., Silva, A. G., Loza, M. I., Kolb, P., Castro, M., and Poso, A. (2016) Structure-based virtual screening for dopamine D2 receptor ligands as potential antipsychotics. *ChemMedChem 11*, 718−729.
(59) Pawley, J. B. (2006) *Handbook of Biological Confocal Microscopy*, 3rd ed., Springer-Verlag, US, Boston.

https://doi.org/10.1021/acschemneuro.0c00647
ACS Chem. Neurosci. 2021, 12, 1313−1327